Object Relative Heading Estimation with Binary Wide Field of View X-Ray Sensing

Andrea López
NASA FINESST Fellow
Graduate Research Assistant
andrea.lopez@colorado.edu

Hanspeter Schaub
Professor and Department Chair
Schaden Leadership Chair

2023 Applied Space Environments Conference
Huntsville, AL, 9-13 October 2023

Ann and H. J. Smead Aerospace
Engineering Sciences Department
University of Colorado, **Boulder**

Motivation

Detecting objects in the vicinity of a spacecraft

- Passive: exploiting space environment interactions
- Regions of interest: GEO, cislunar
- Applications:
  - Artificial/natural debris: detect and track in situ
  - Proximity operations: On Orbit Servicing, Assembly and Manufacturing (OSAM)

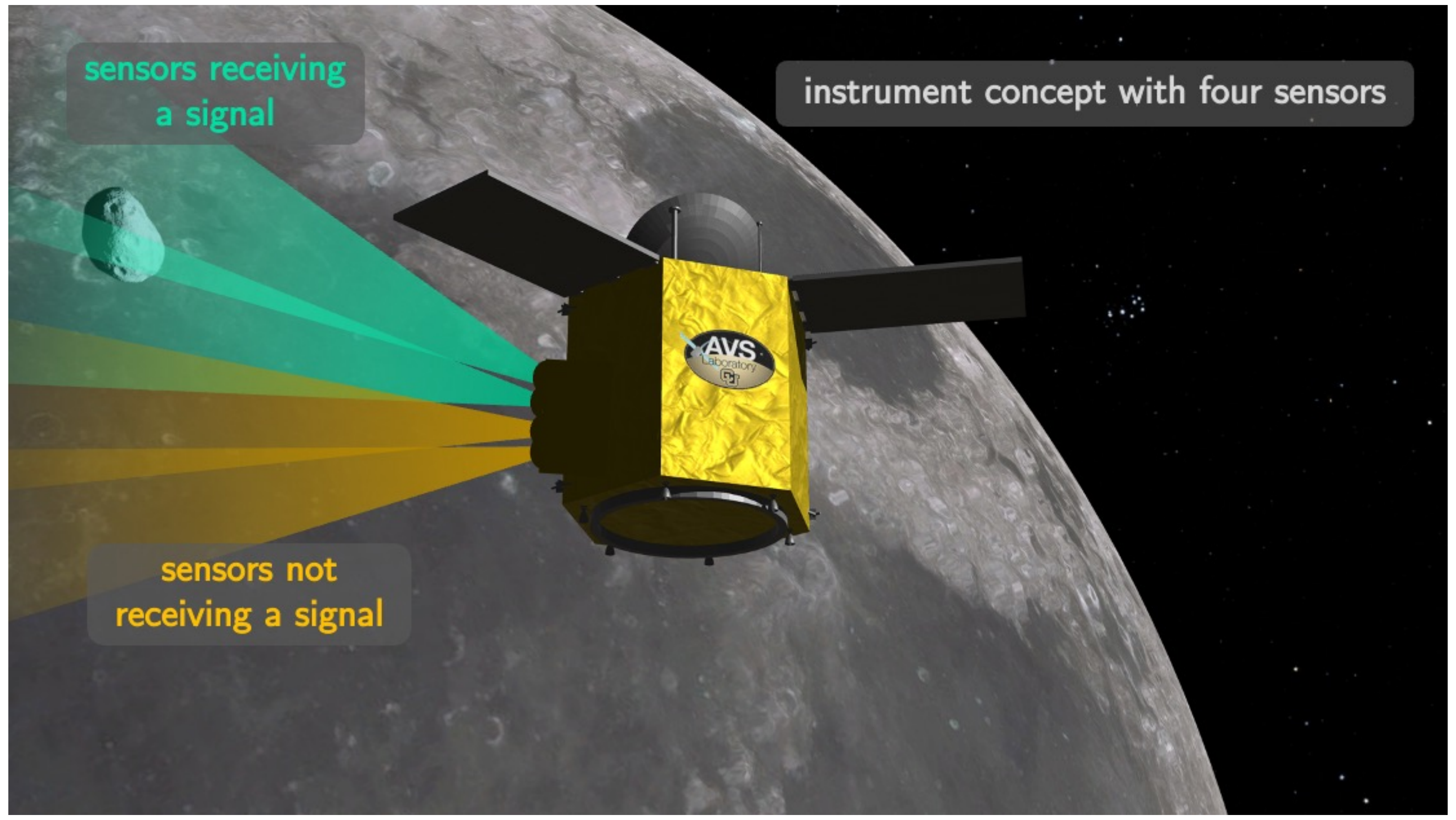

Ambient generated x-rays

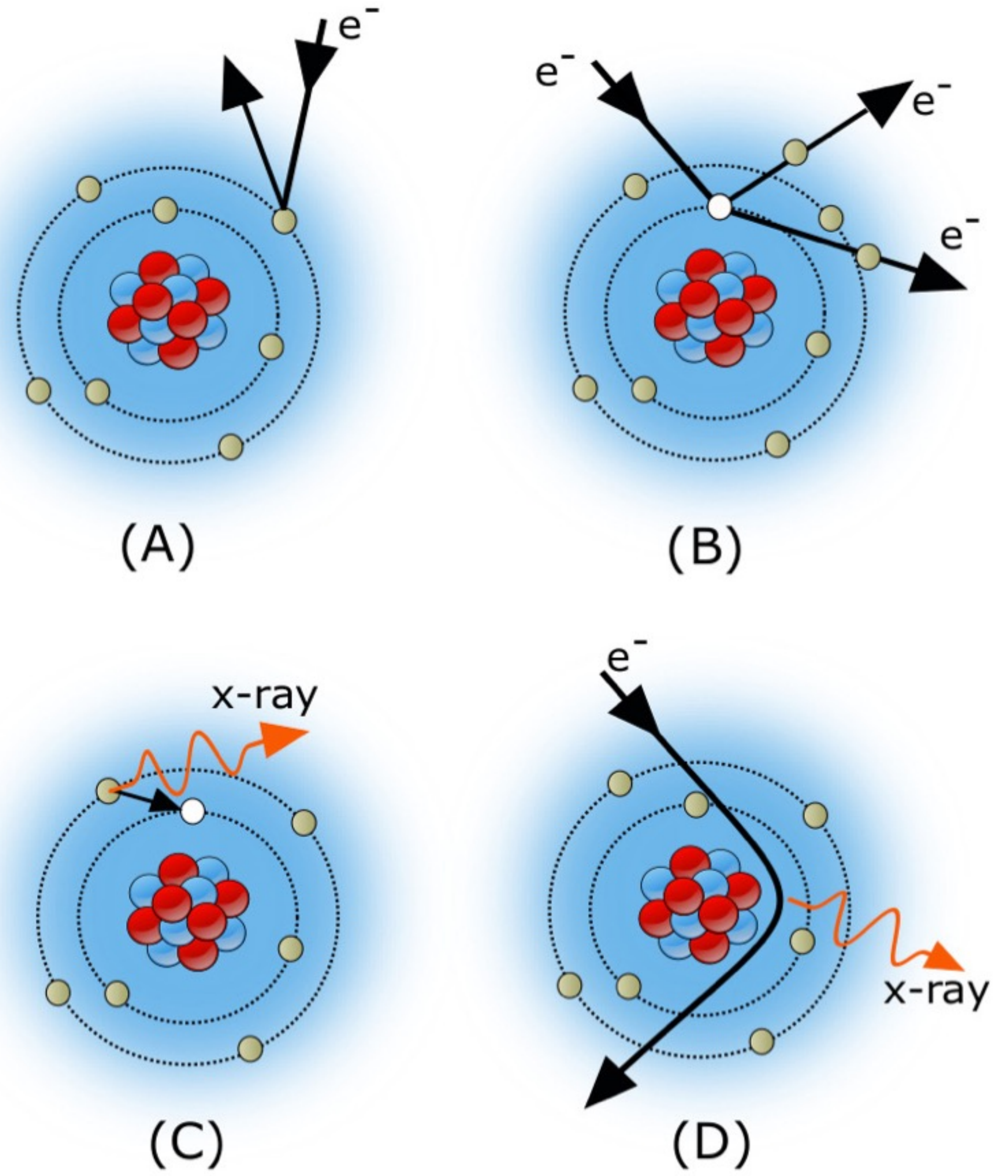

(A) Backscatter; (B) secondary electrons;
(C) characteristic x-rays; (D) bremsstrahlung x-rays

Wilson, K. and Schaub, H., 2019. X-ray spectroscopy for electrostatic potential and material determination of space objects. *IEEE Transactions on Plasma Science*, *47*(8), pp.3858-3866.

Problem Statement

Coarse Sun Sensor (CSS) assembly

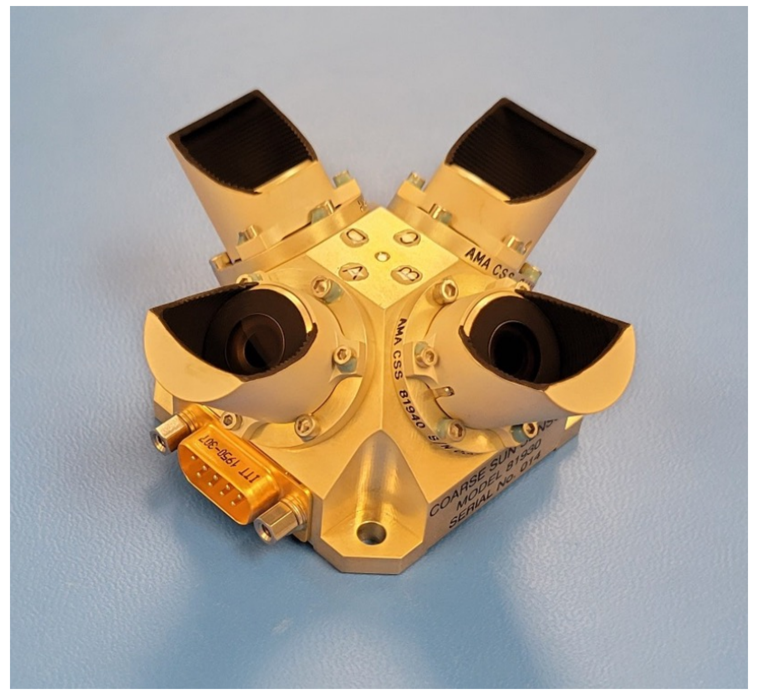

CSS pyramid

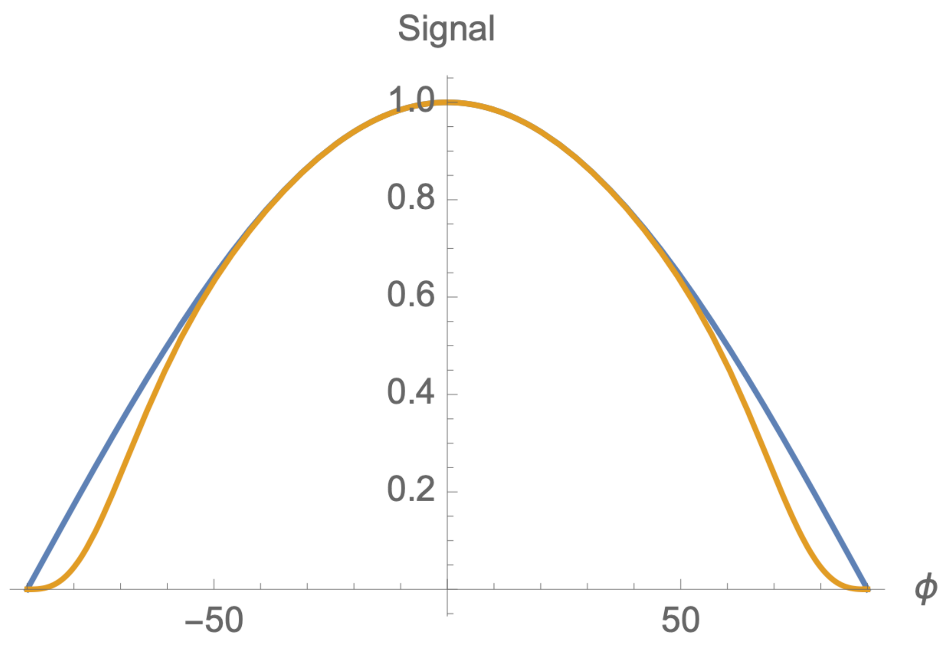

Cosine law (blue) and typical CSS behavior (orange)

X-ray Sensors: COTS, 15 deg FOV

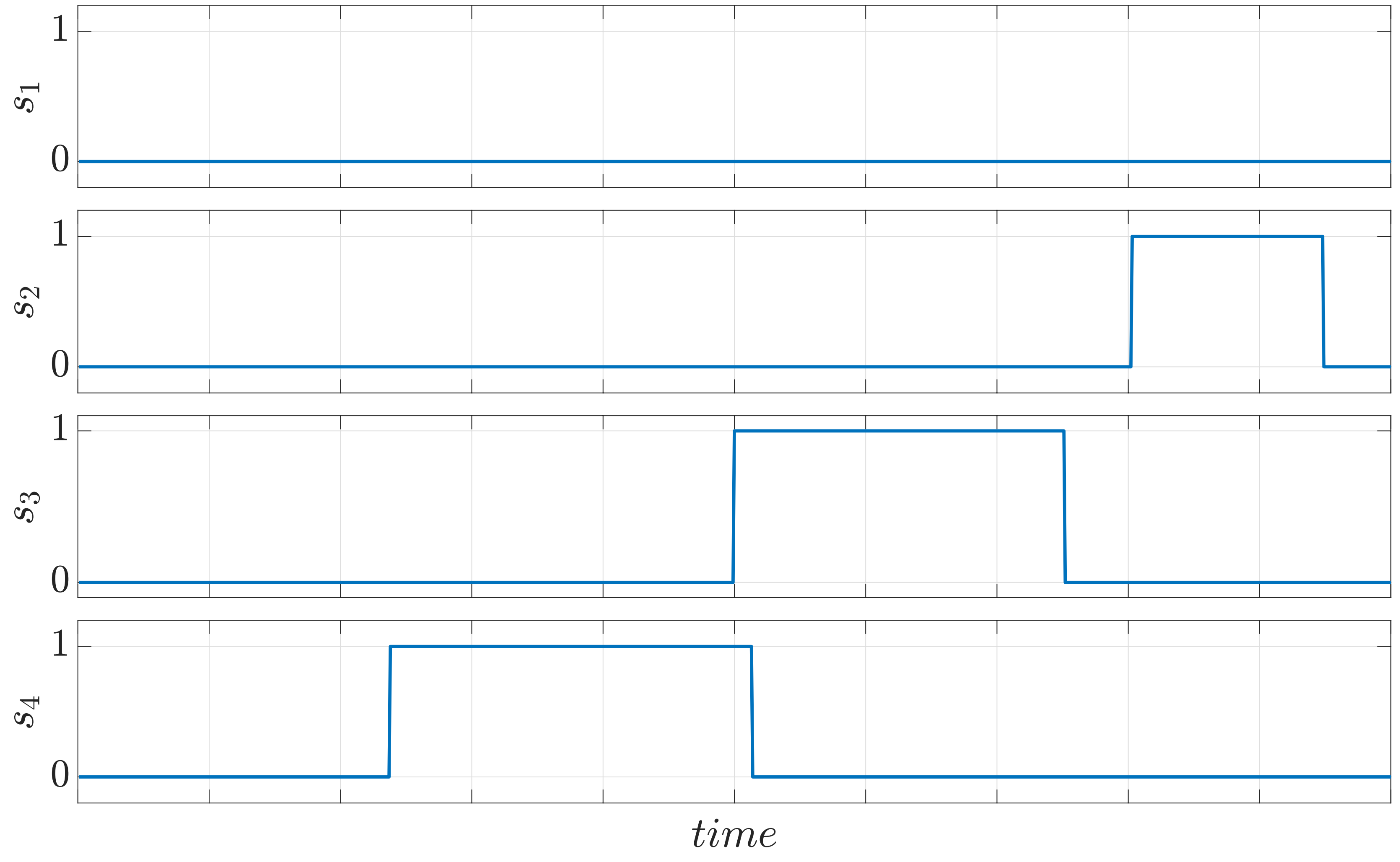

Signal acquisition/loss at edge of FOV

$$\boldsymbol{m}^T\boldsymbol{h} = \cos f$$

Peak intensity is not known → only *on* or *off* information

Testing on/off hypothesis

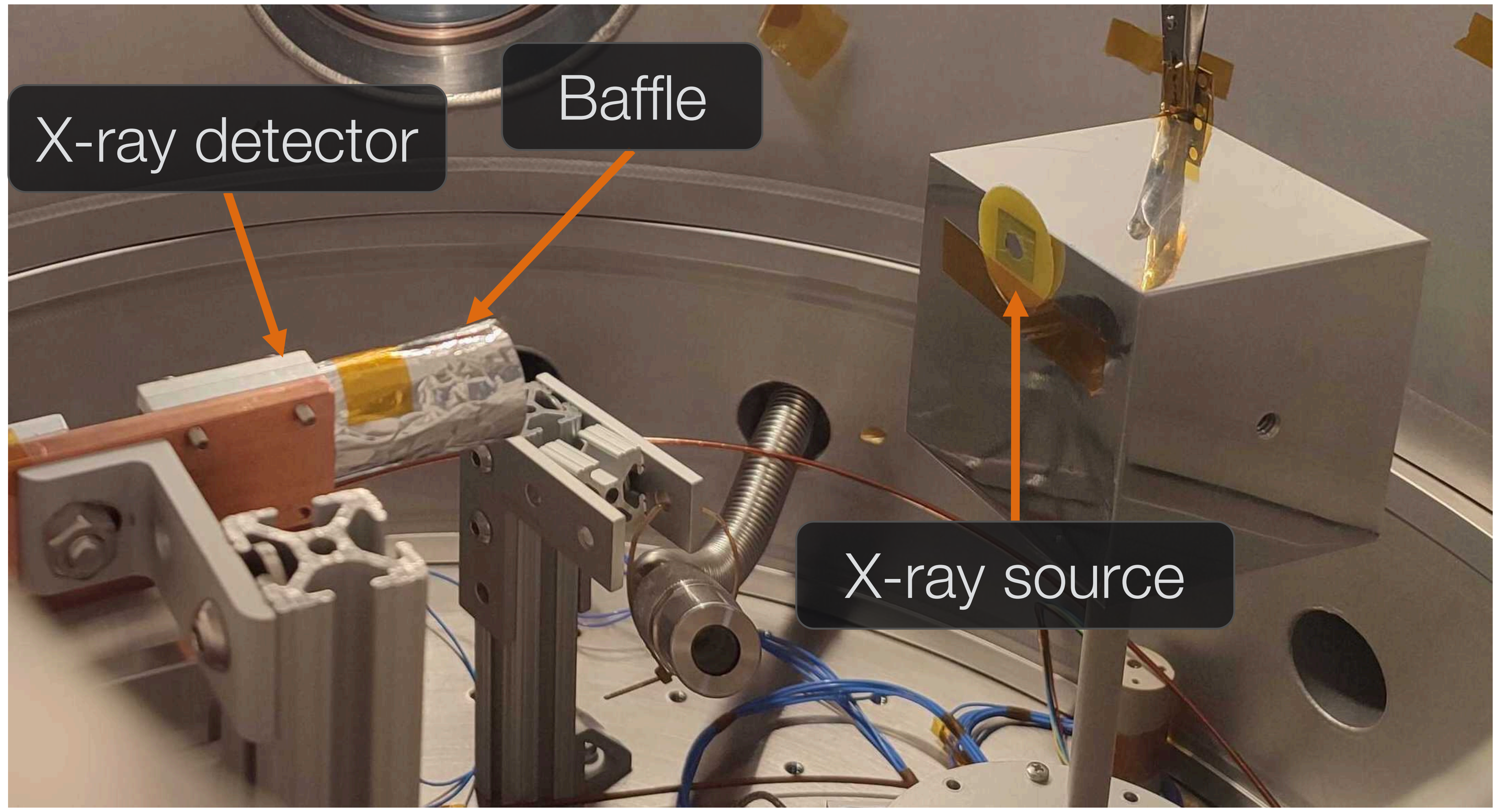

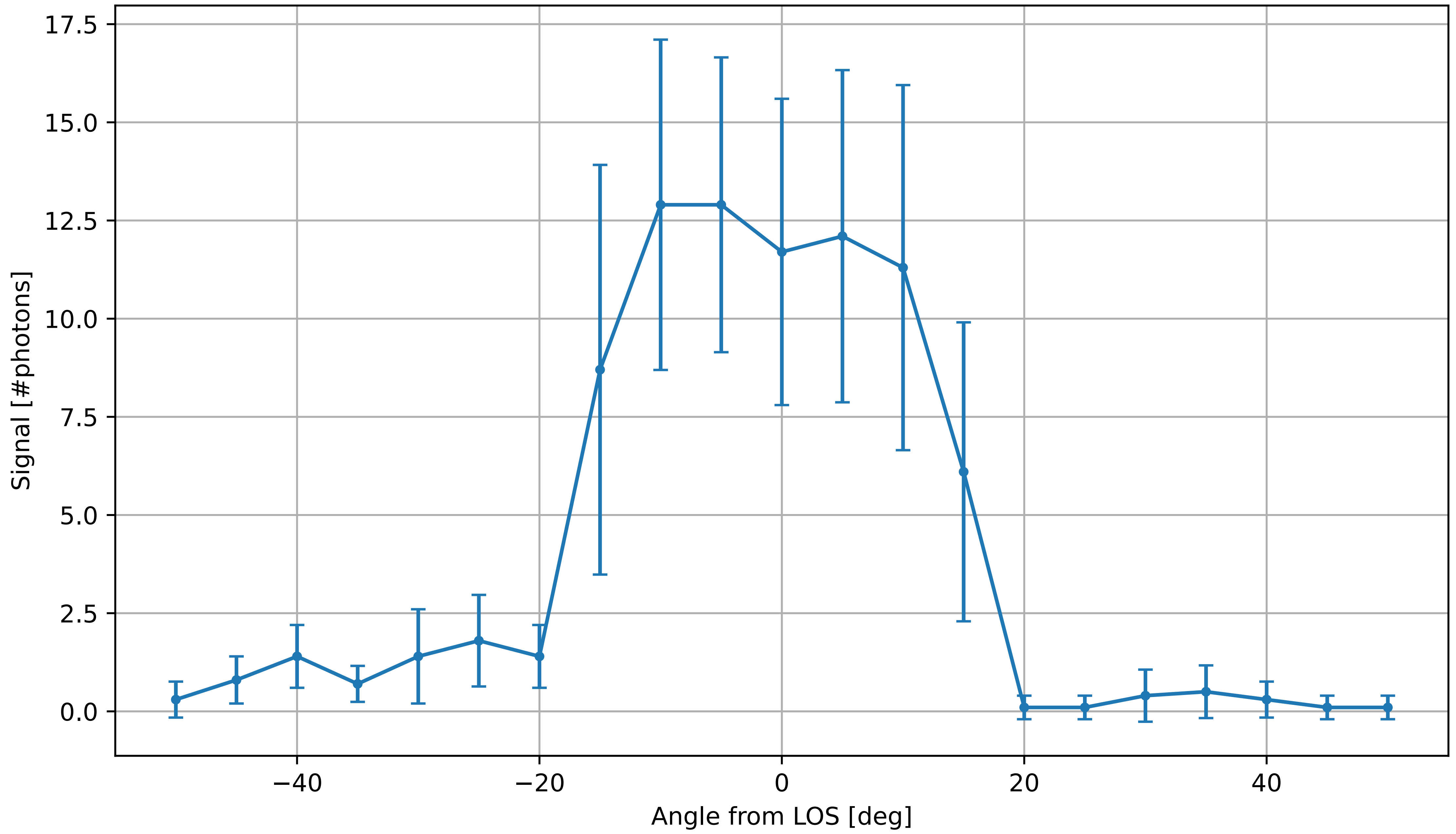

Problem Statement: Trigger events

Sensor configuration

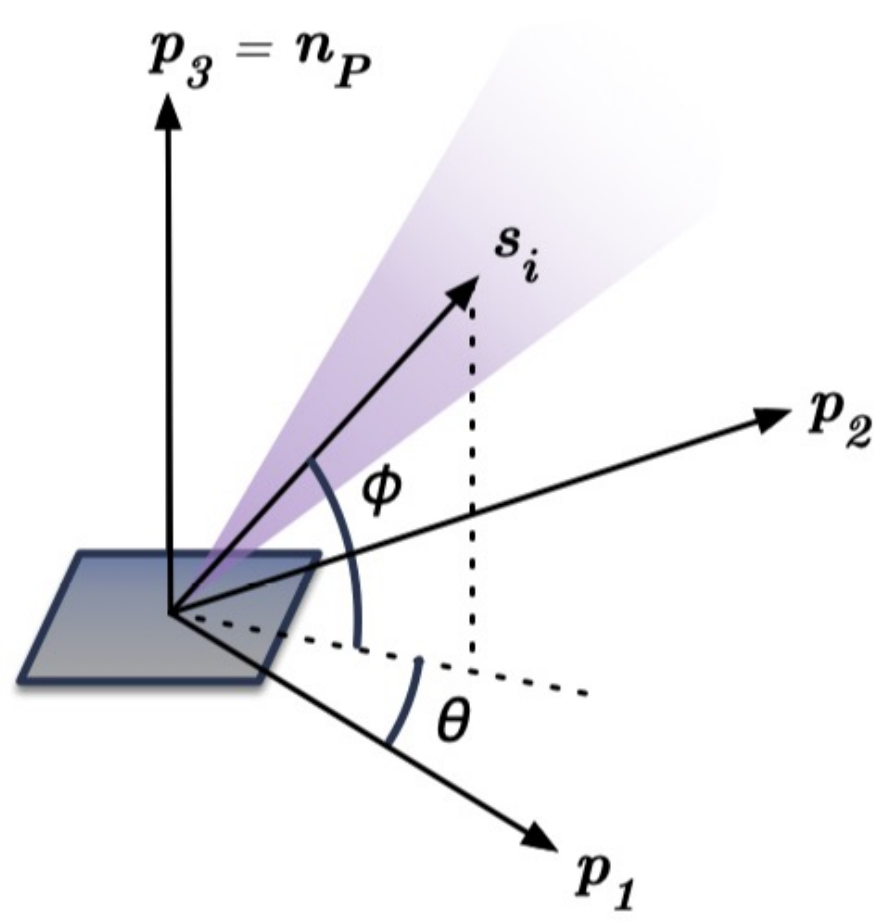

Rotating platform

$$\boldsymbol{\omega} = \omega \boldsymbol{p}_3$$

López, A., Hammerl, J., and Schaub, H., "Detecting Space Objects With Binary Wide Field Of View X-Ray Sensing," AAS Astrodynamics Specialist Conference, Charlotte, NC, 2022. Paper No. AAS 22-602

Static target: heading

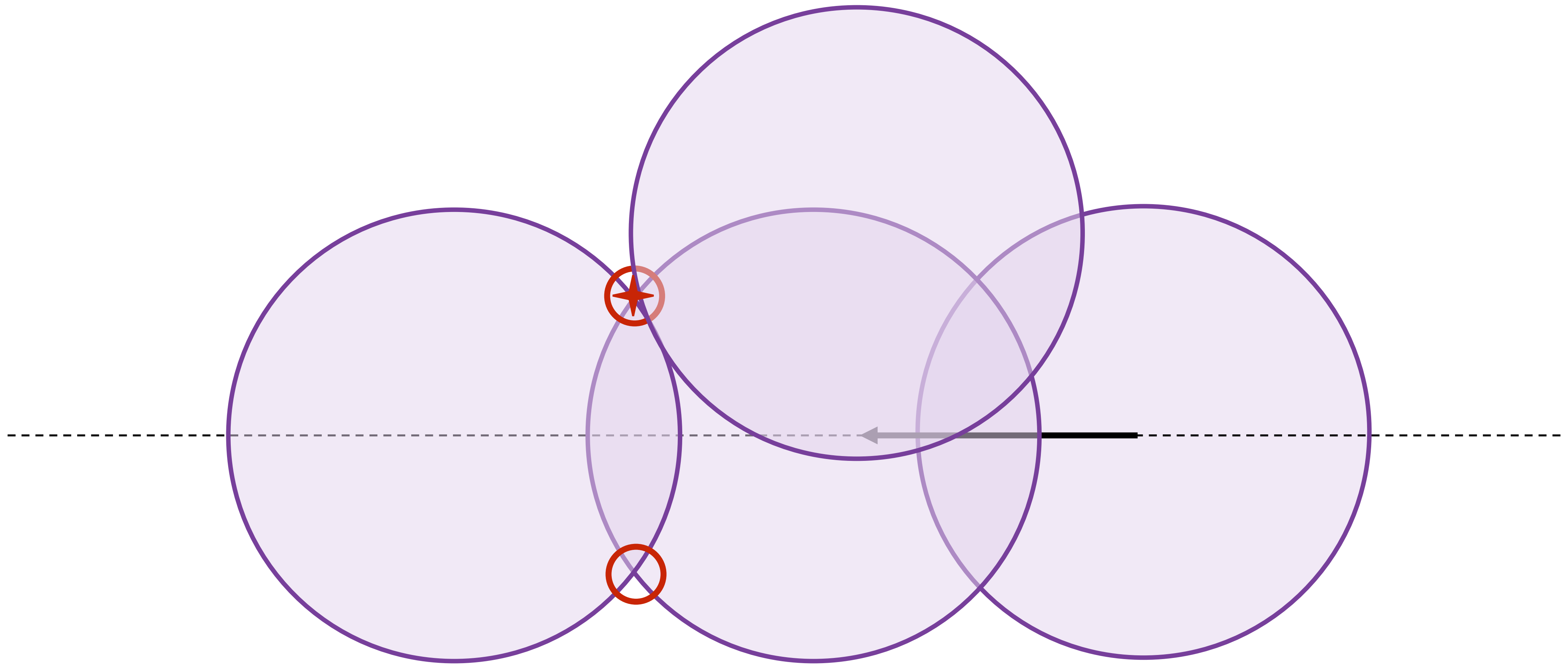

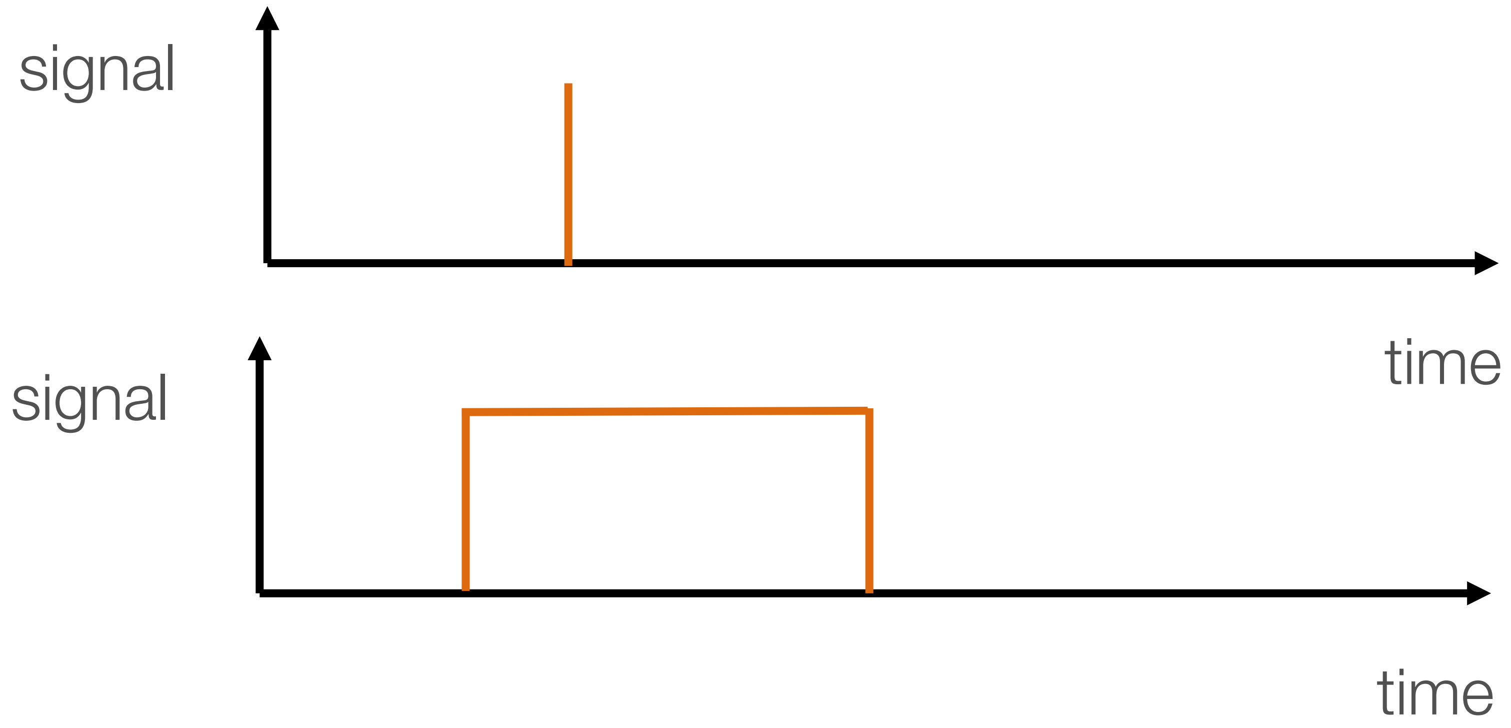

Need events from multiple sensors to disambiguate

Problem Statement: Configuration

CSS-like configuration

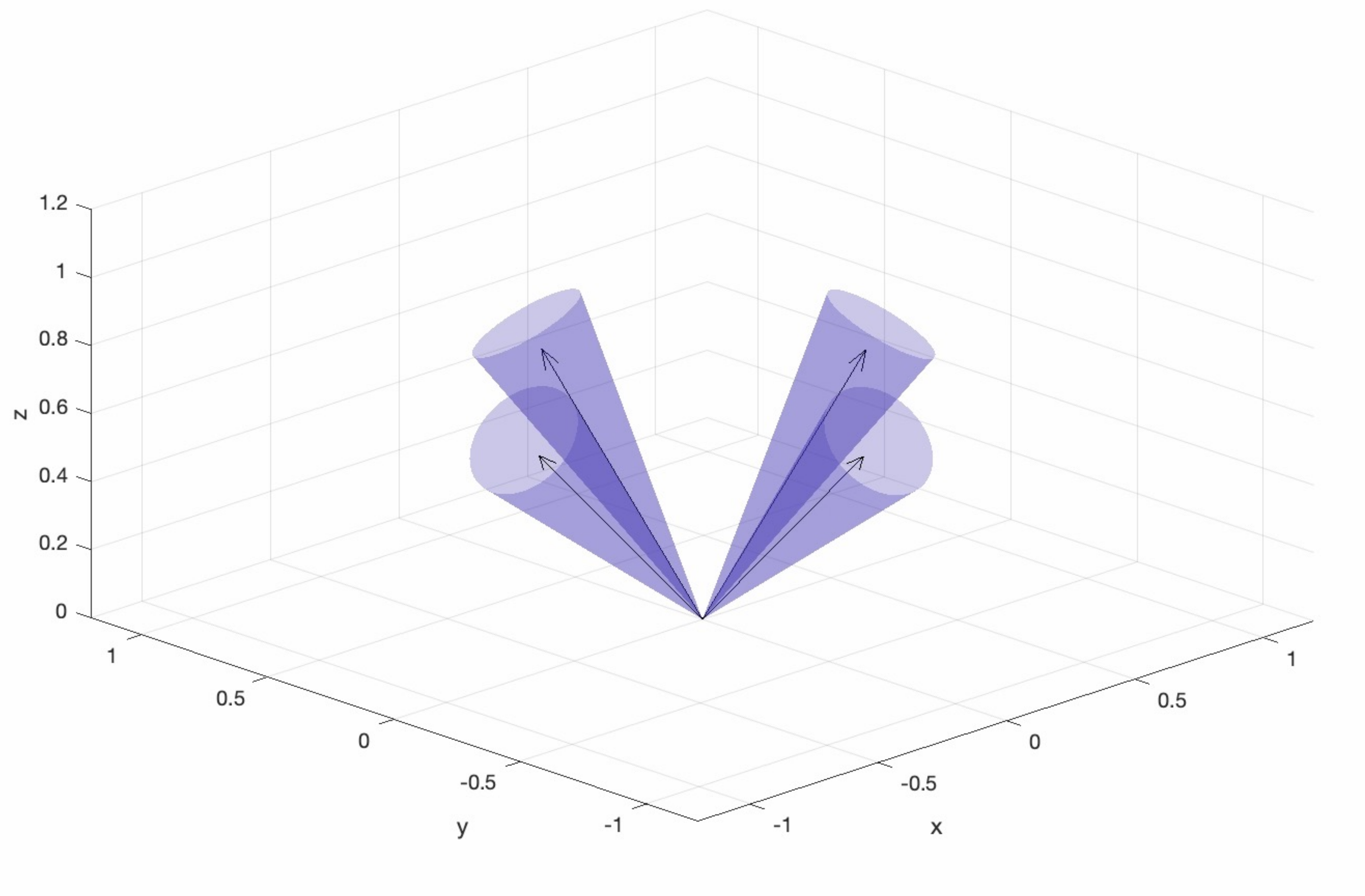

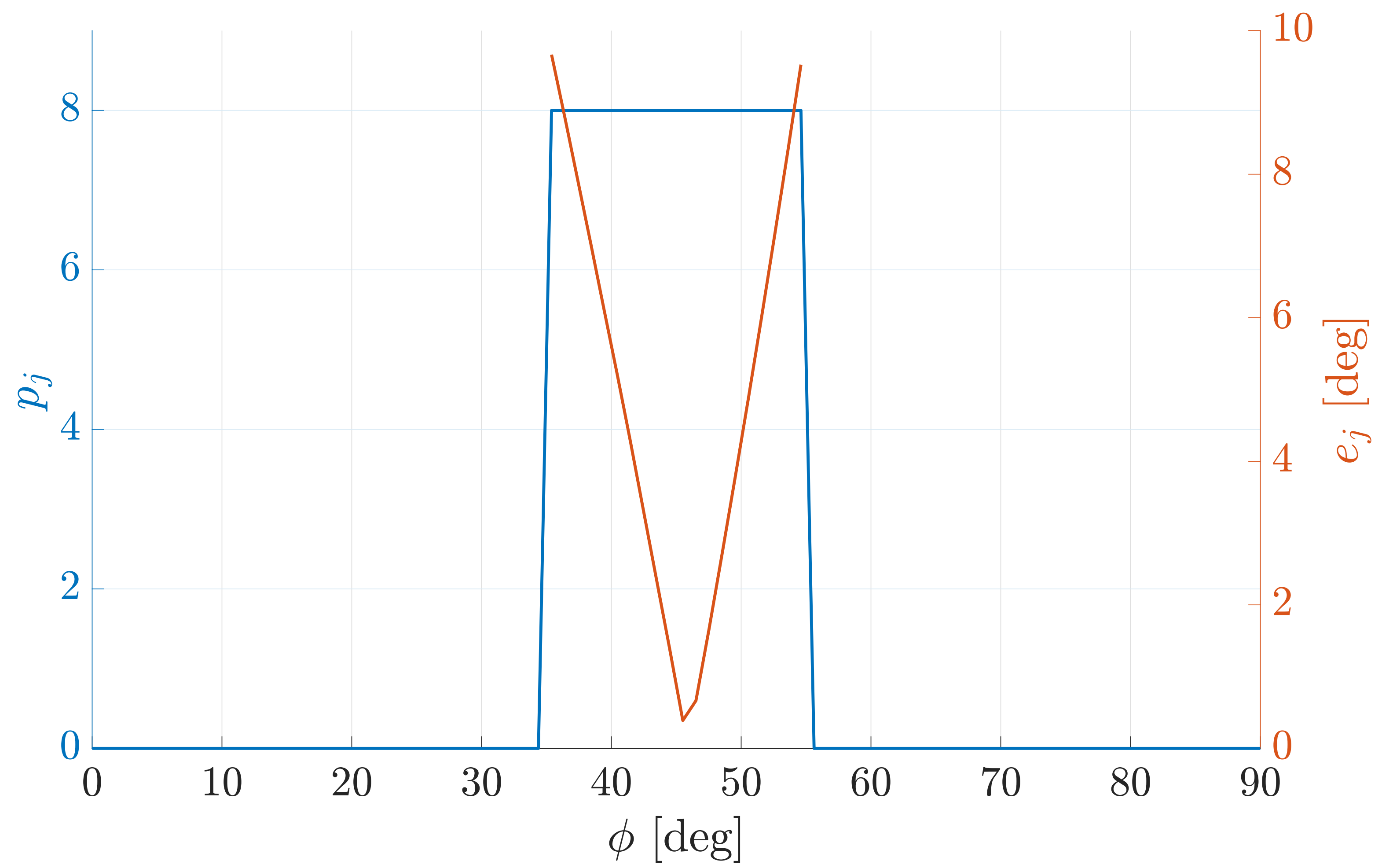

Rotating platform

$$\boldsymbol{\omega} = \omega \hat{\boldsymbol{p}}_3$$

López, A., Hammerl, J., and Schaub, H., "Detecting Space Objects With Binary Wide Field Of View X-Ray Sensing," AAS Astrodynamics Specialist Conference, Charlotte, NC, 2022. Paper No. AAS 22-602

Only two unique measurements: under-determined problem

Problem Statement: Configuration

Elevation distributed configuration

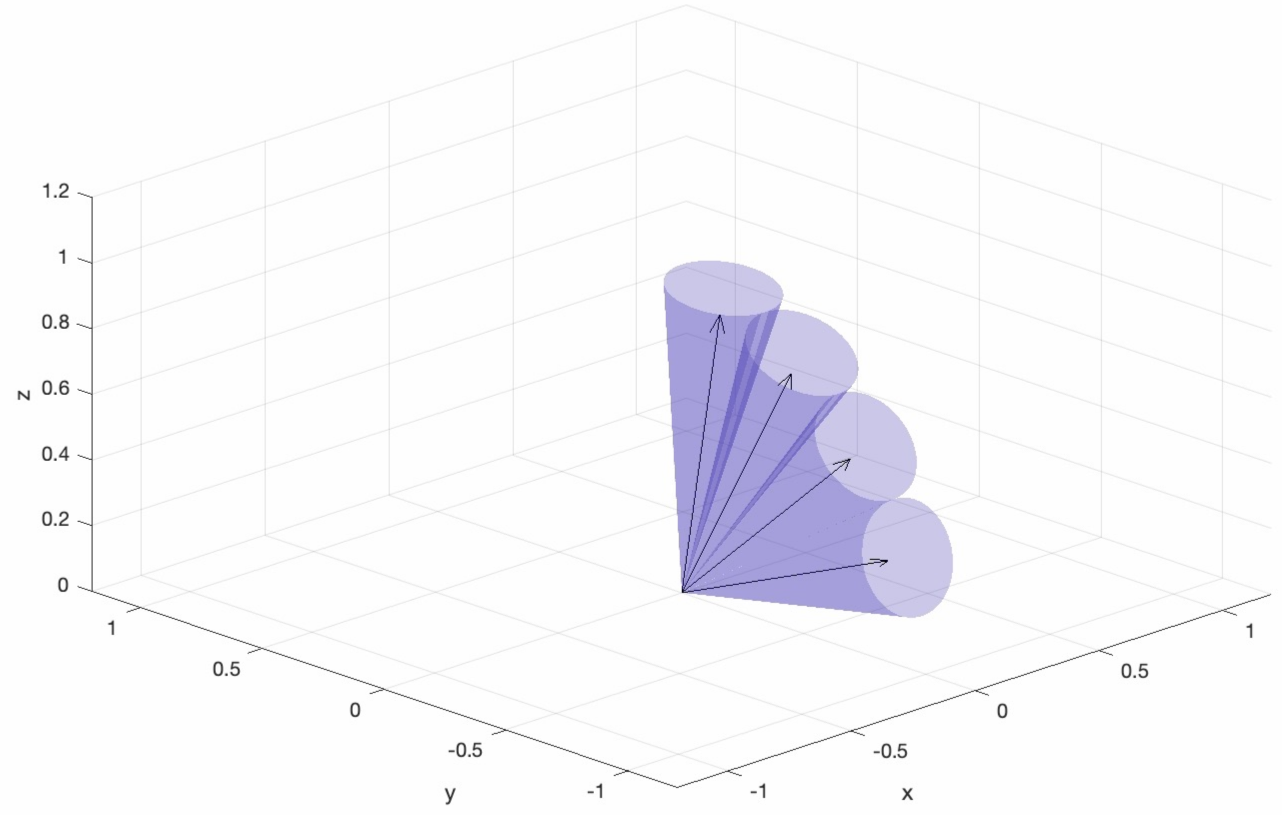

No sensor overlap

Under-determined

Maximize coverage

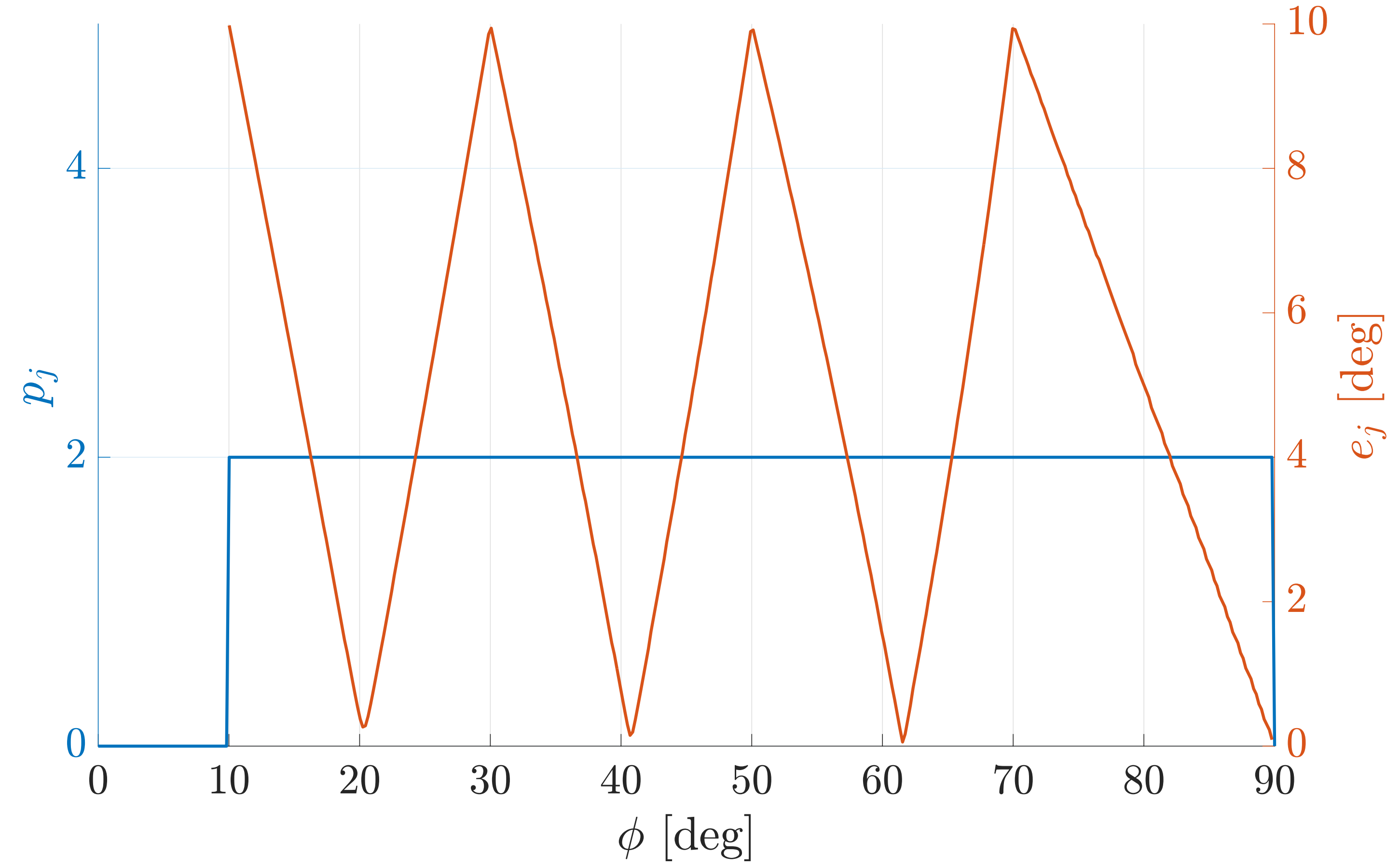

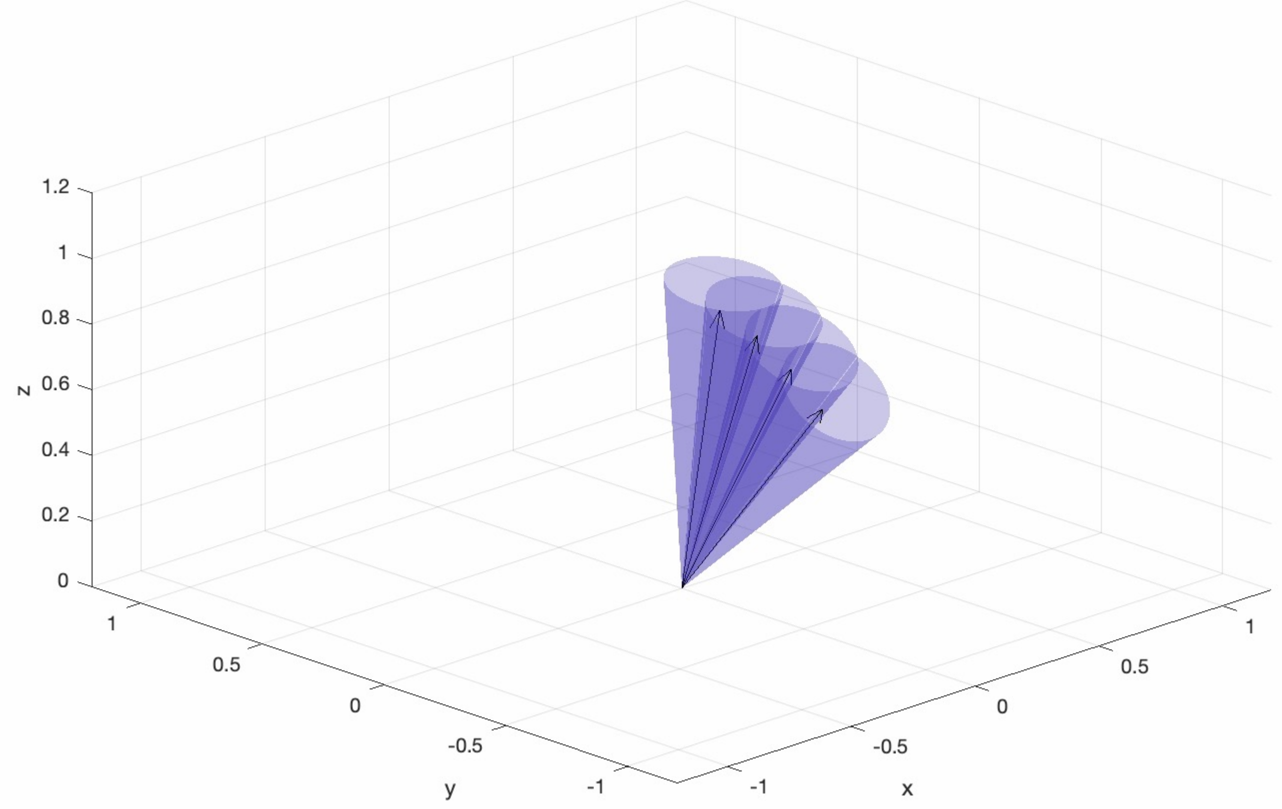

Sensor overlap

Only under-determined at edges

Minimize error

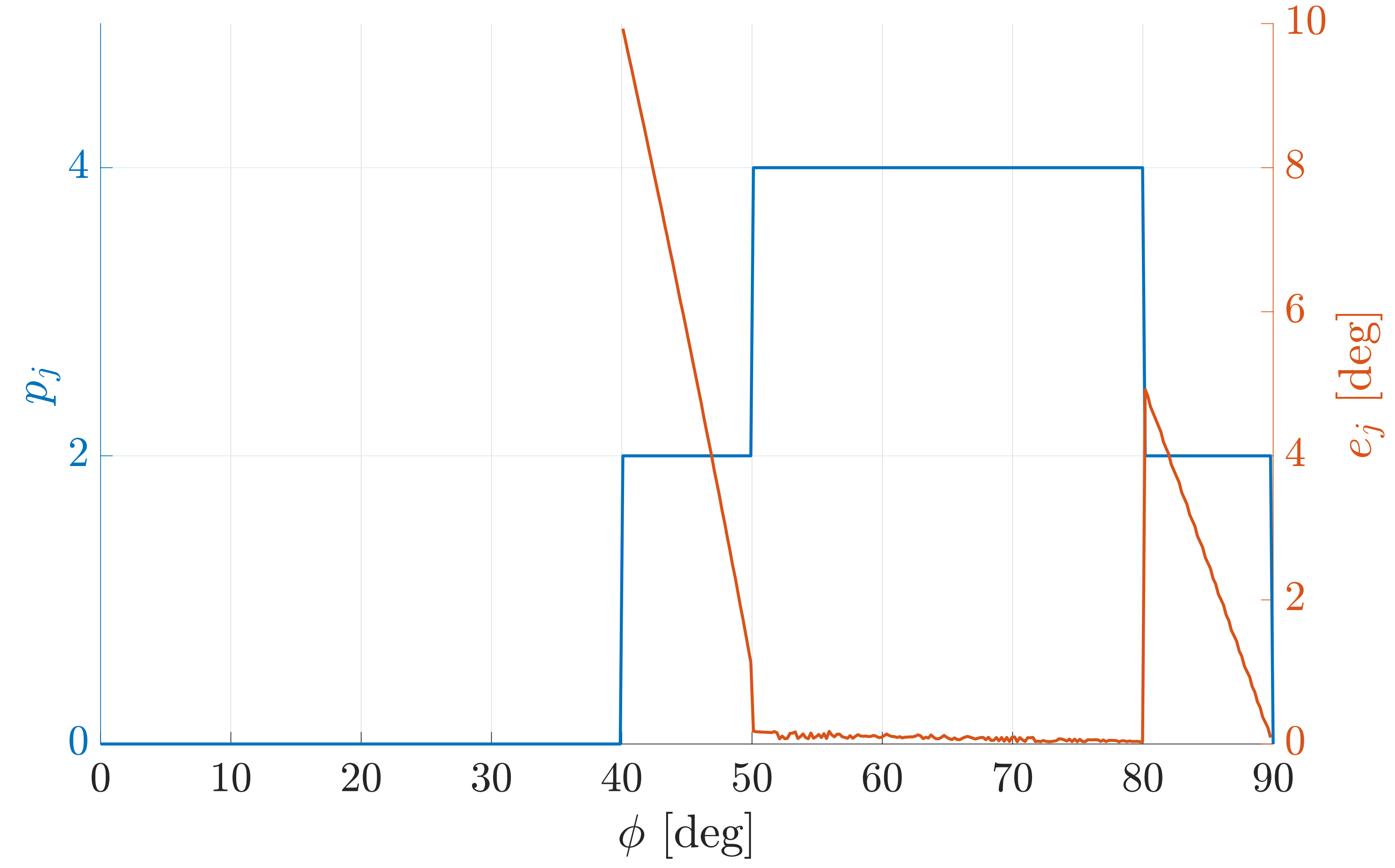

Problem Statement: Configuration

Sensor configuration

Sensor	θ [deg]	ϕ [deg]
1	0	0
2	0	15
3	0	30
4	0	45
5	0	60
6	0	75

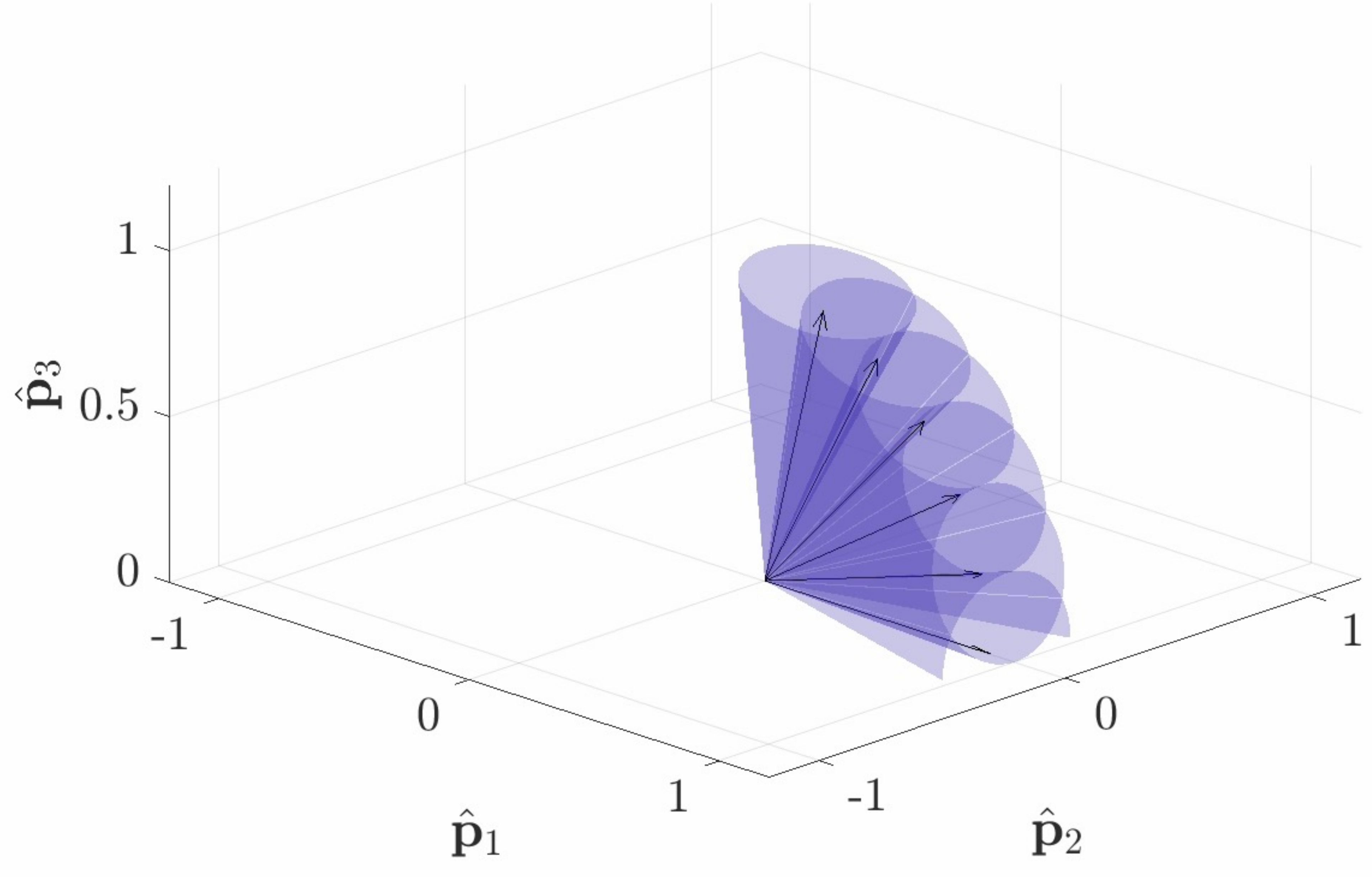

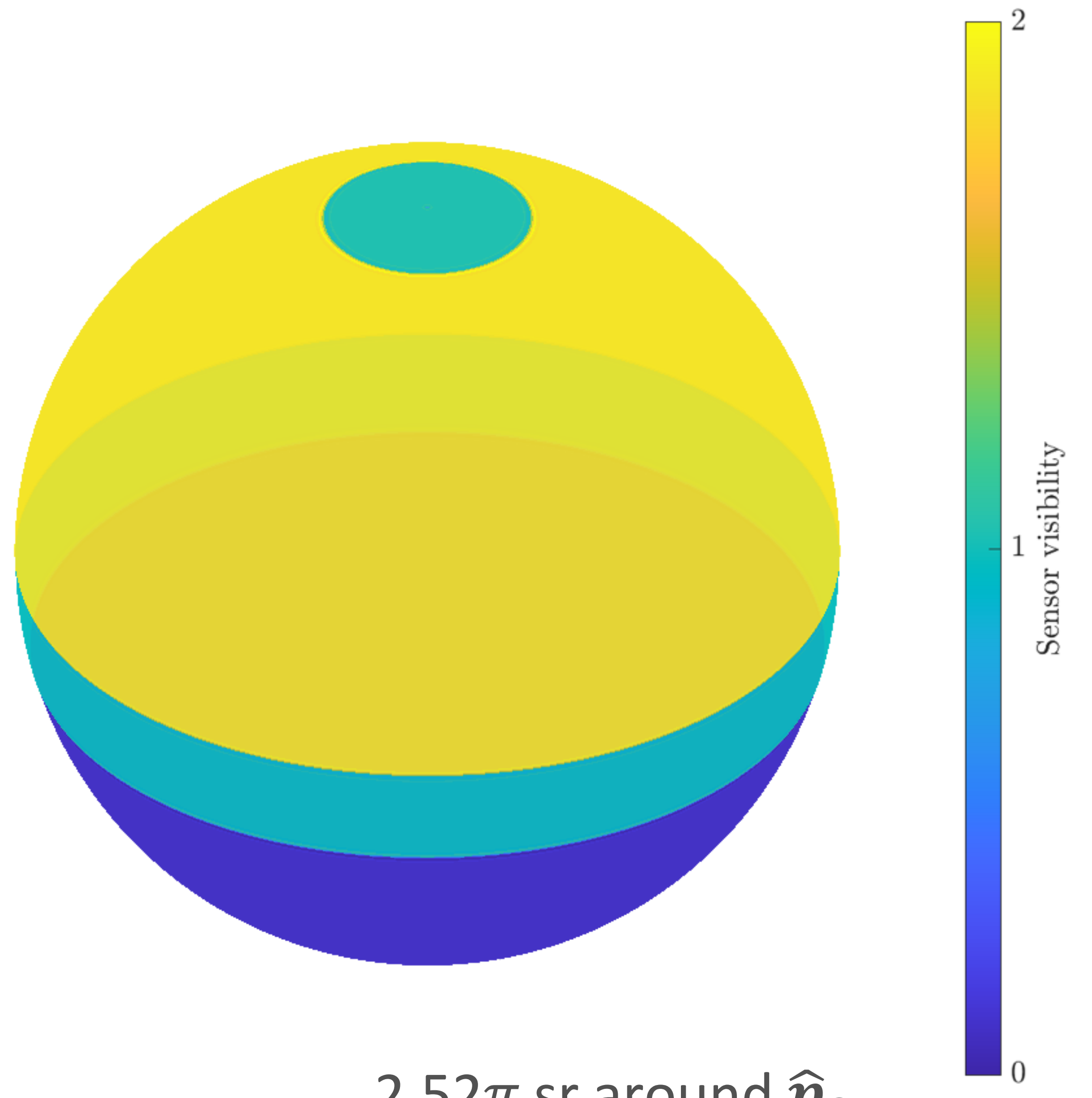

2.52π sr around $\hat{\boldsymbol{p}}_3$
1.93π sr with 2 sensor

Rotating platform

$$\boldsymbol{\omega} = \omega \hat{\boldsymbol{p}}_3$$

López, A., Hammerl, J., and Schaub, H., "Detecting Space Objects With Binary Wide Field Of View X-Ray Sensing," AAS Astrodynamics Specialist Conference, Charlotte, NC, 2022. Paper No. AAS 22-602

Rotating, partially overlapping sensors

Problem Statement: Multiple clusters

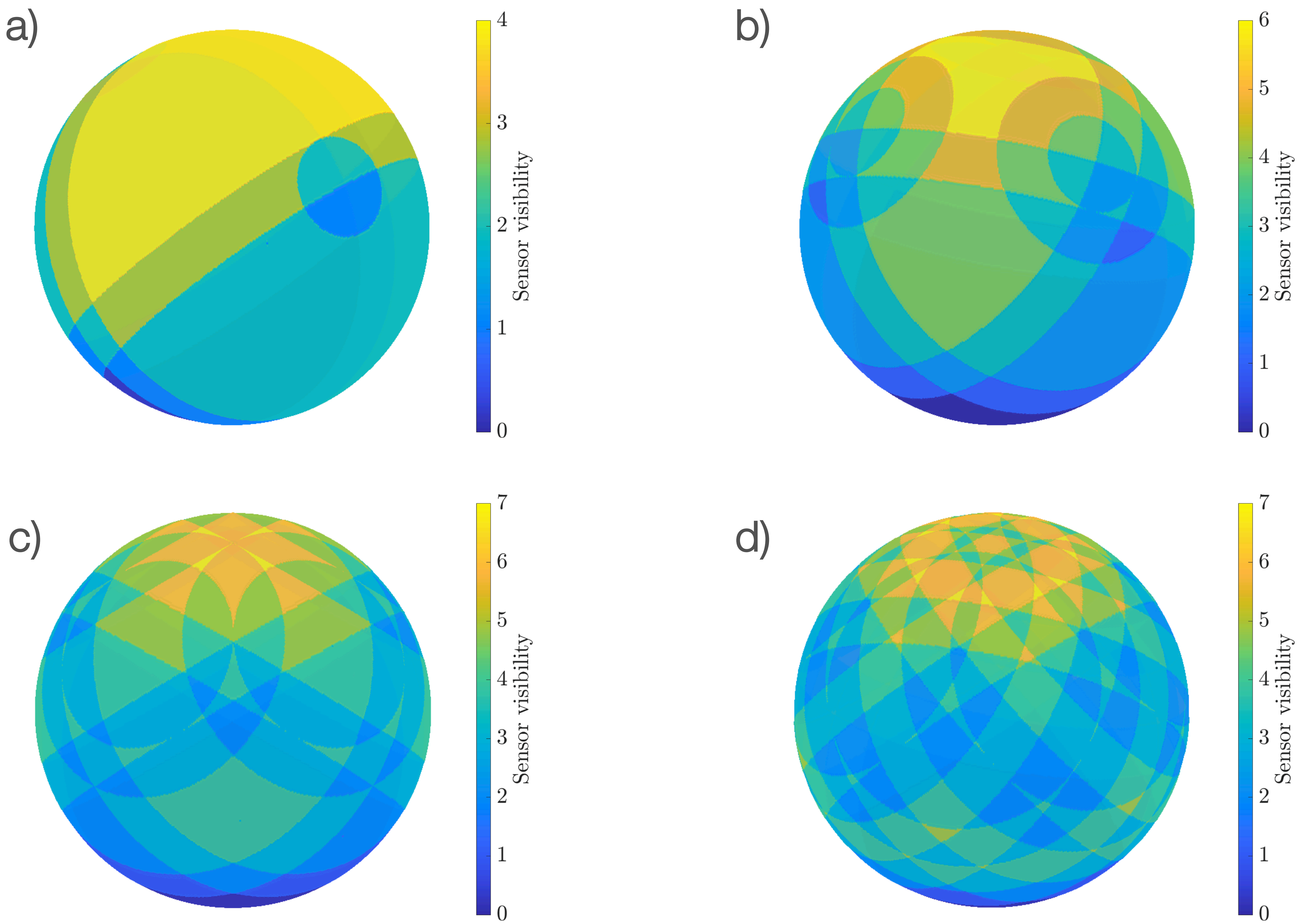

a) Two six-sensor clusters
b) Three four-sensor clusters
c) Four three-sensor clusters
d) Six two-sensor clusters

López, A., Hammerl, J., and Schaub, H., “Detecting Space Objects With Binary Wide Field Of View X-Ray Sensing,” AAS Astrodynamics Specialist Conference, Charlotte, NC, 2022. Paper No. AAS 22-602

Relative Orbit Cases

$$\boldsymbol{x}_{\boldsymbol{\infty},c} = (a = 32434\text{ km}, e = 0.3, i = 10°, \Omega = 120°, \omega = 10°, M = 180°)^T$$

Table 1: Relative orbit cases description in classic element differences

	Δa [km]	Δe	Δi [rad]	$\Delta\omega$ [rad]	$\Delta\Omega$ [rad]	ΔM_0 [rad]
Case 1	-1.5e-1	5e-5	5e-4	1.5e-4	1.5e-4	-1.5e-3
Case 2	0	0	0	0	0	-3e-3

Case 1

Safety ellipse drifting orbit

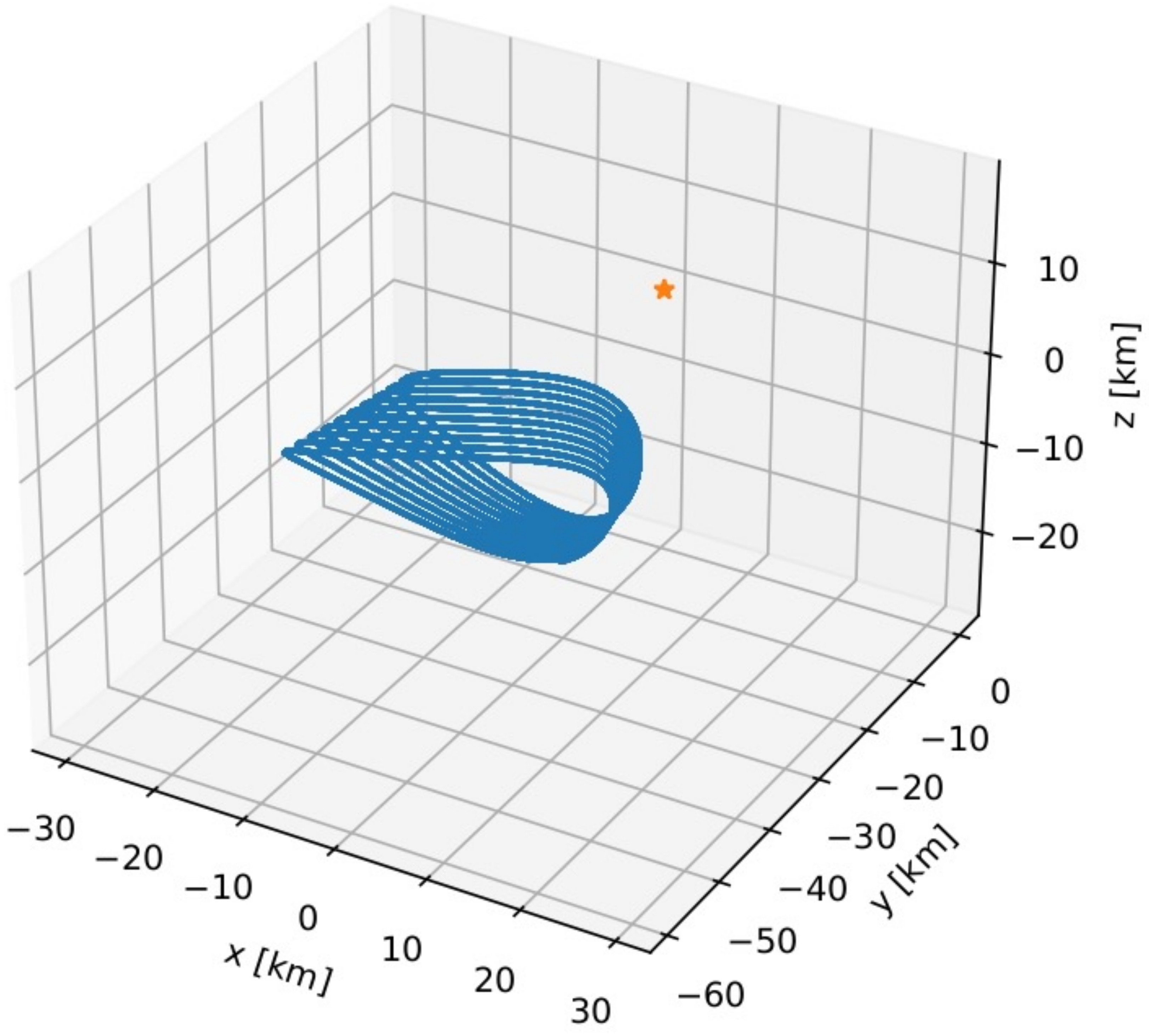

Hill frame

Case 2

Lead-follower

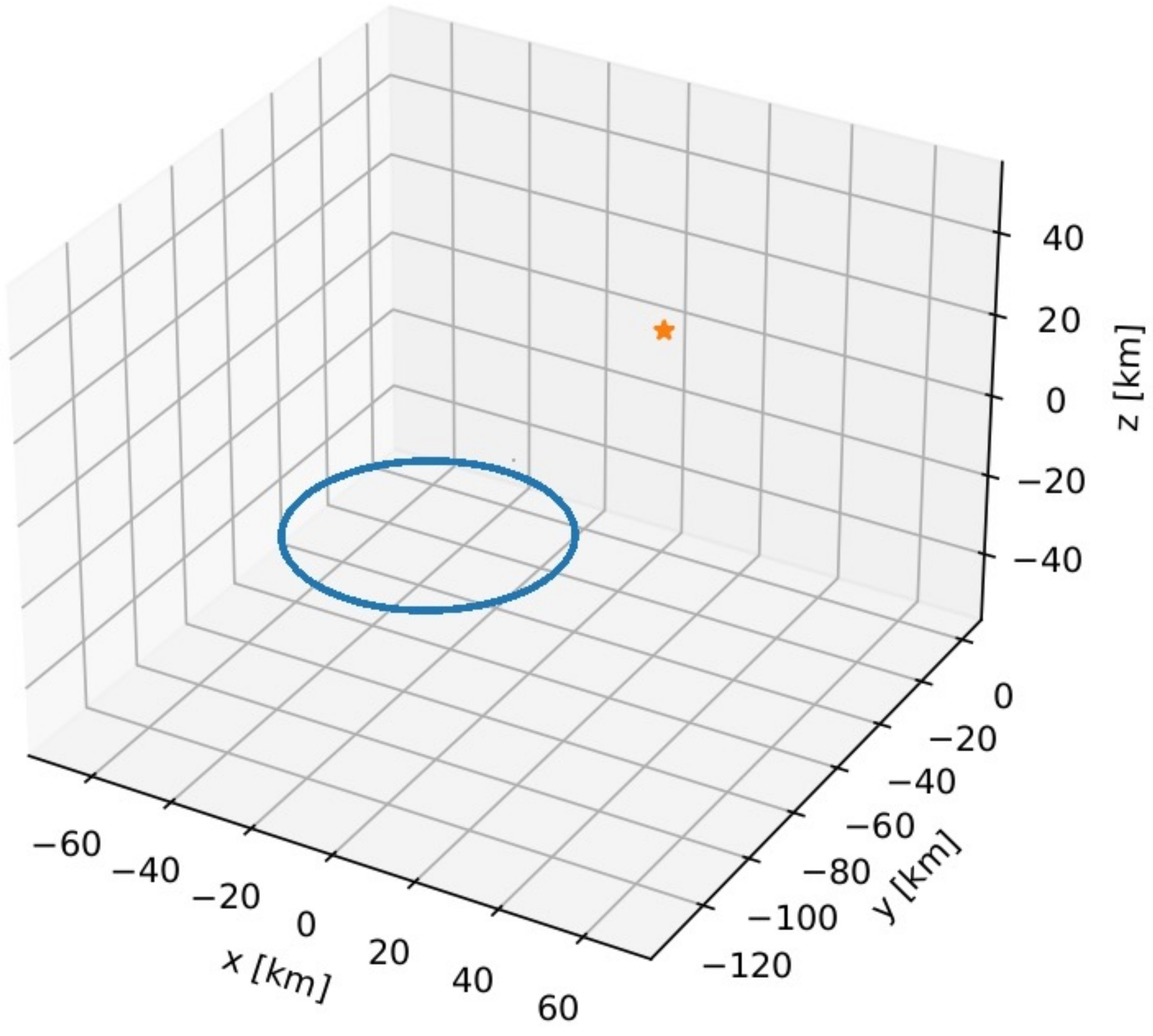

Batch pre-processing

Signal acquisition/loss:

$$\boldsymbol{m}_i^T(t_i)\boldsymbol{h}(t_i) = \cos f$$

Combining events $\boldsymbol{m}_i(t_i)$ after one platform revolution:

$$\begin{bmatrix} \boldsymbol{m}_1^T(t_1) \\ \boldsymbol{m}_2^T(t_2) \\ \dots \\ \boldsymbol{m}_p^T(t_p) \end{bmatrix} \boldsymbol{h}\,(t^*) = \begin{bmatrix} \cos f \\ \cos f \\ \dots \\ \cos f \end{bmatrix}$$

Solving for $\bar{\boldsymbol{h}}(\bar{t})$:

$$\bar{\boldsymbol{h}} = \begin{bmatrix} \boldsymbol{m}_1^T(t_1) \\ \boldsymbol{m}_2^T(t_2) \\ \dots \\ \boldsymbol{m}_p^T(t_p) \end{bmatrix}^+ \begin{bmatrix} \cos f \\ \cos f \\ \dots \\ \cos f \end{bmatrix}$$

$$\bar{t} = \frac{1}{p}\sum_{i=1}^{p} t_i$$

Measurement:

$$y = \begin{pmatrix} \theta \\ \varepsilon \end{pmatrix} = \begin{pmatrix} \arctan({}^{\mathcal{P}}h_2 / {}^{\mathcal{P}}h_1) \\ \arcsin({}^{\mathcal{P}}h_3) \end{pmatrix}$$

Batch pre-processing

Static target case:

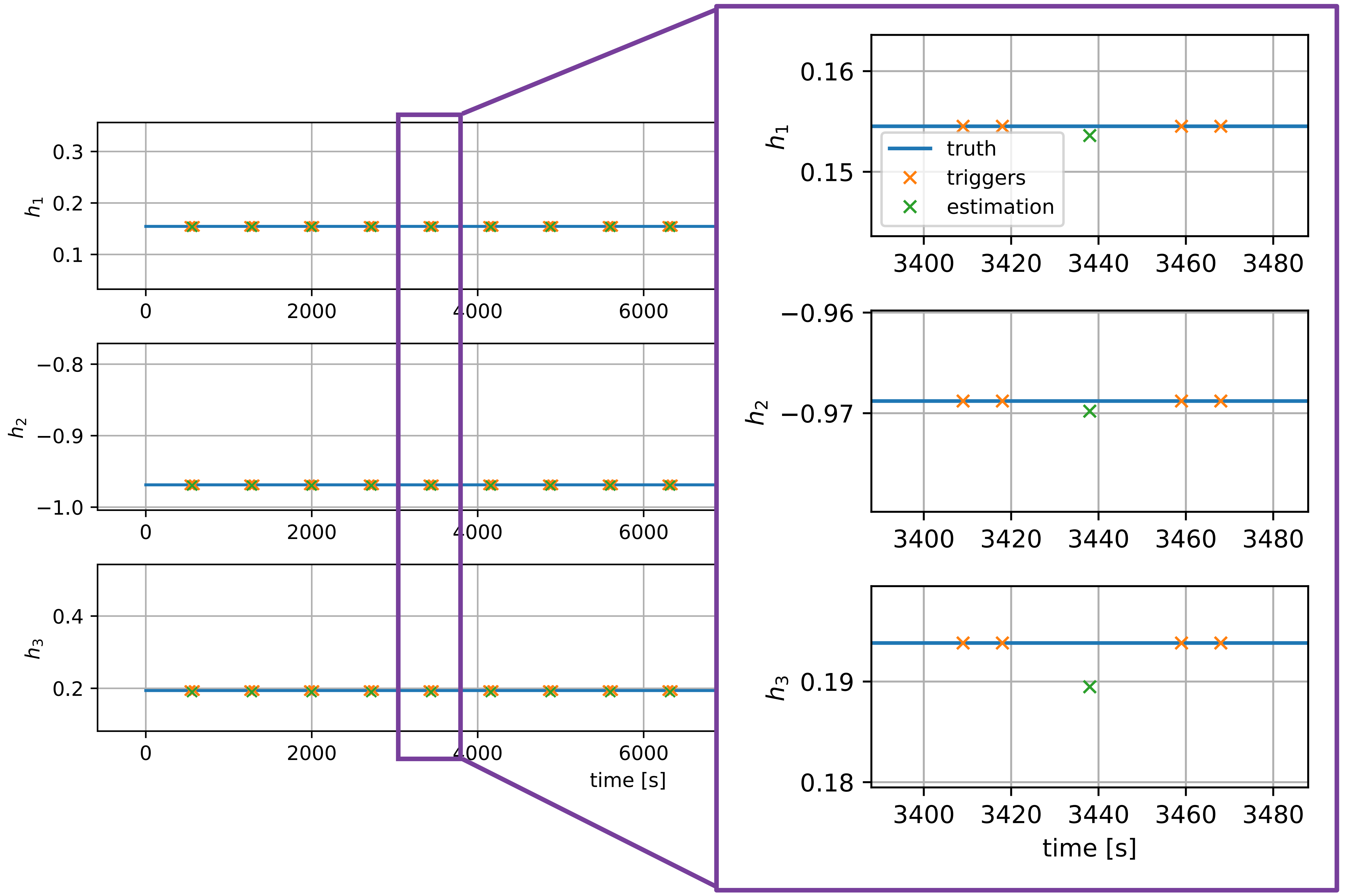

Relative orbit case (case 1):

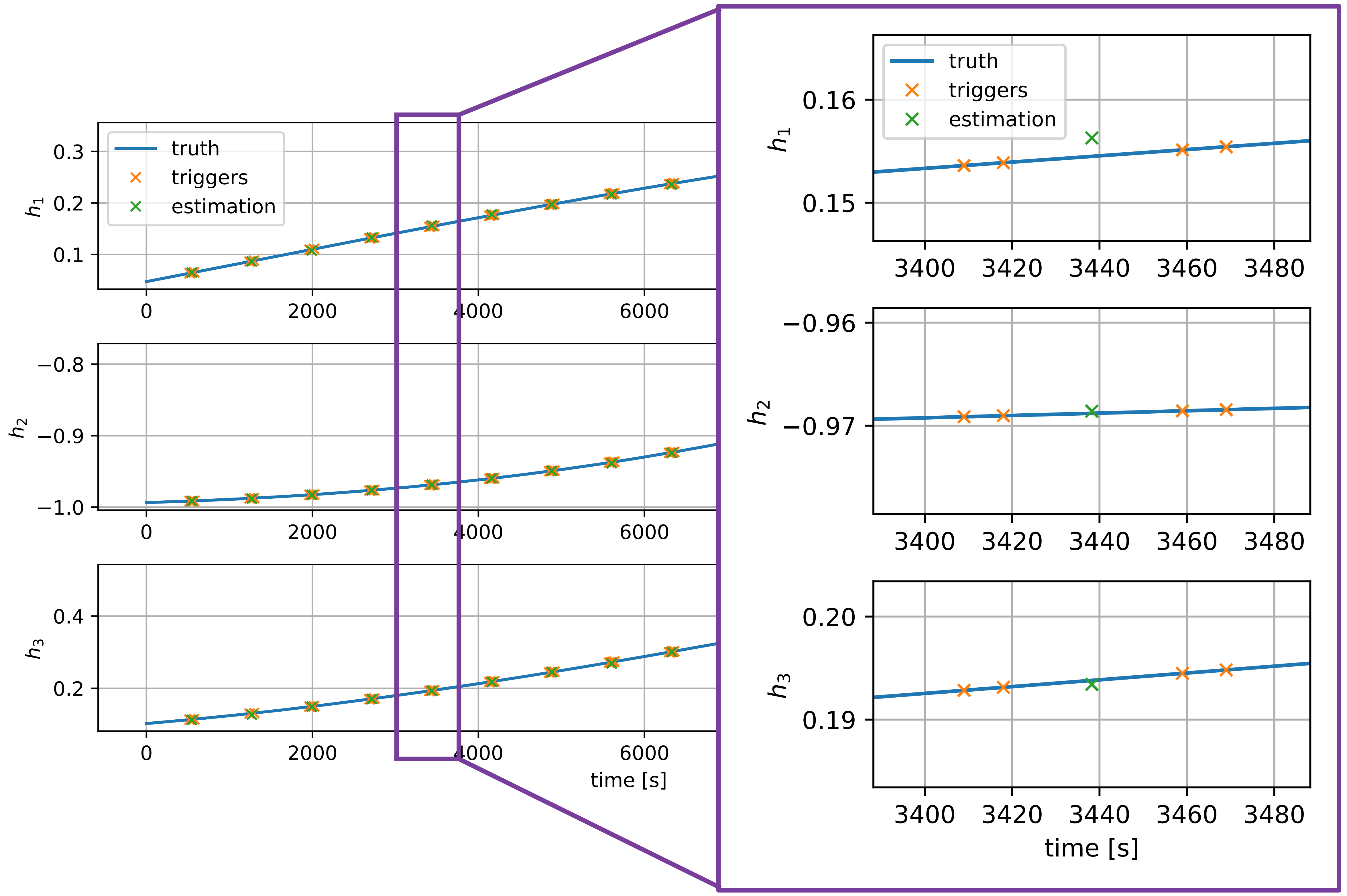

Error is linked to precision in knowledge of sensor pointing and target motion

Heading estimation: error statistics

Sampling every 1s

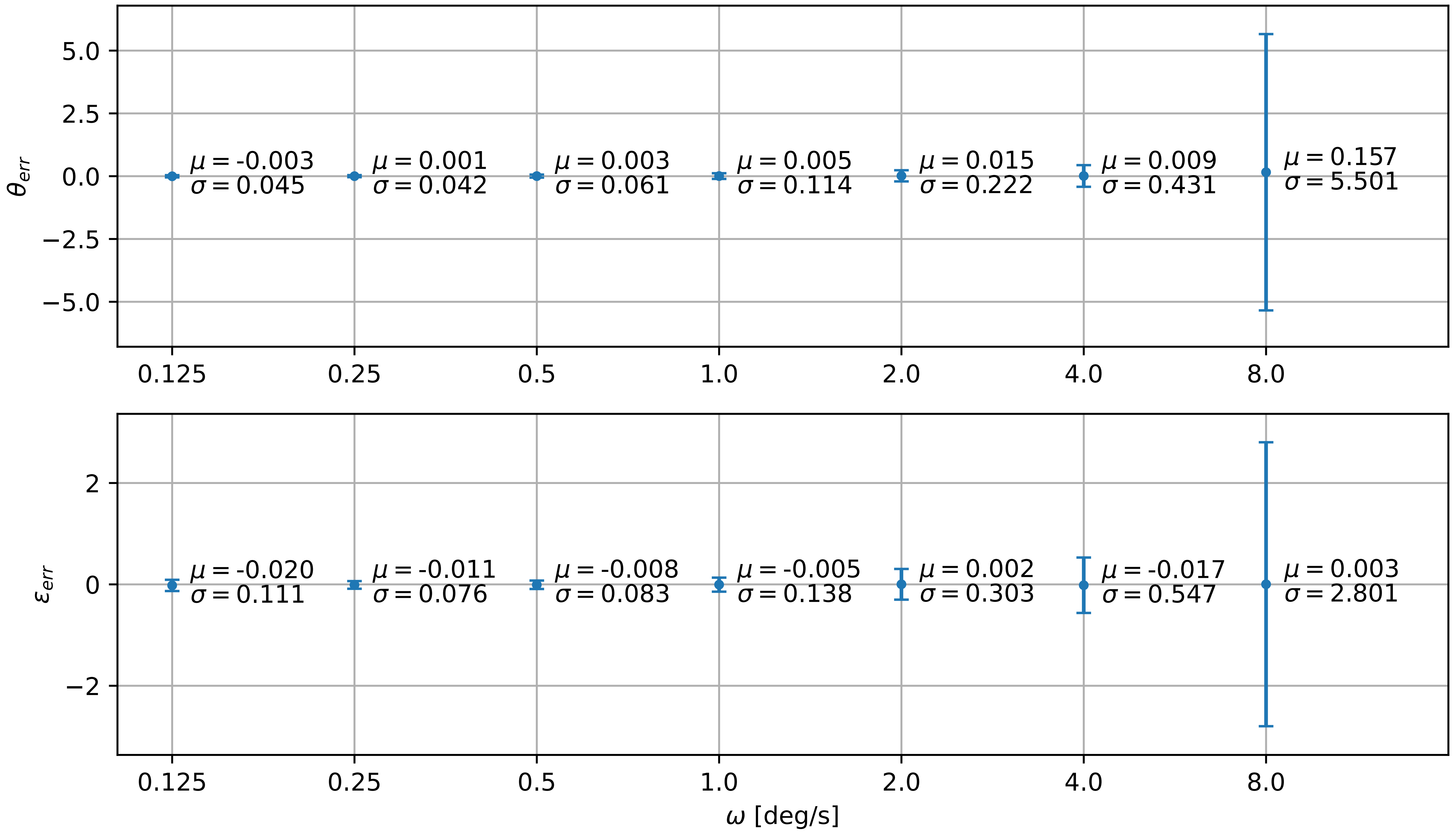

To reduce error in sensor pointing knowledge:

- Reducing platform angular speed
- Reducing sampling time

Relative Orbit Estimation: Case 1

Perfect bearing angles

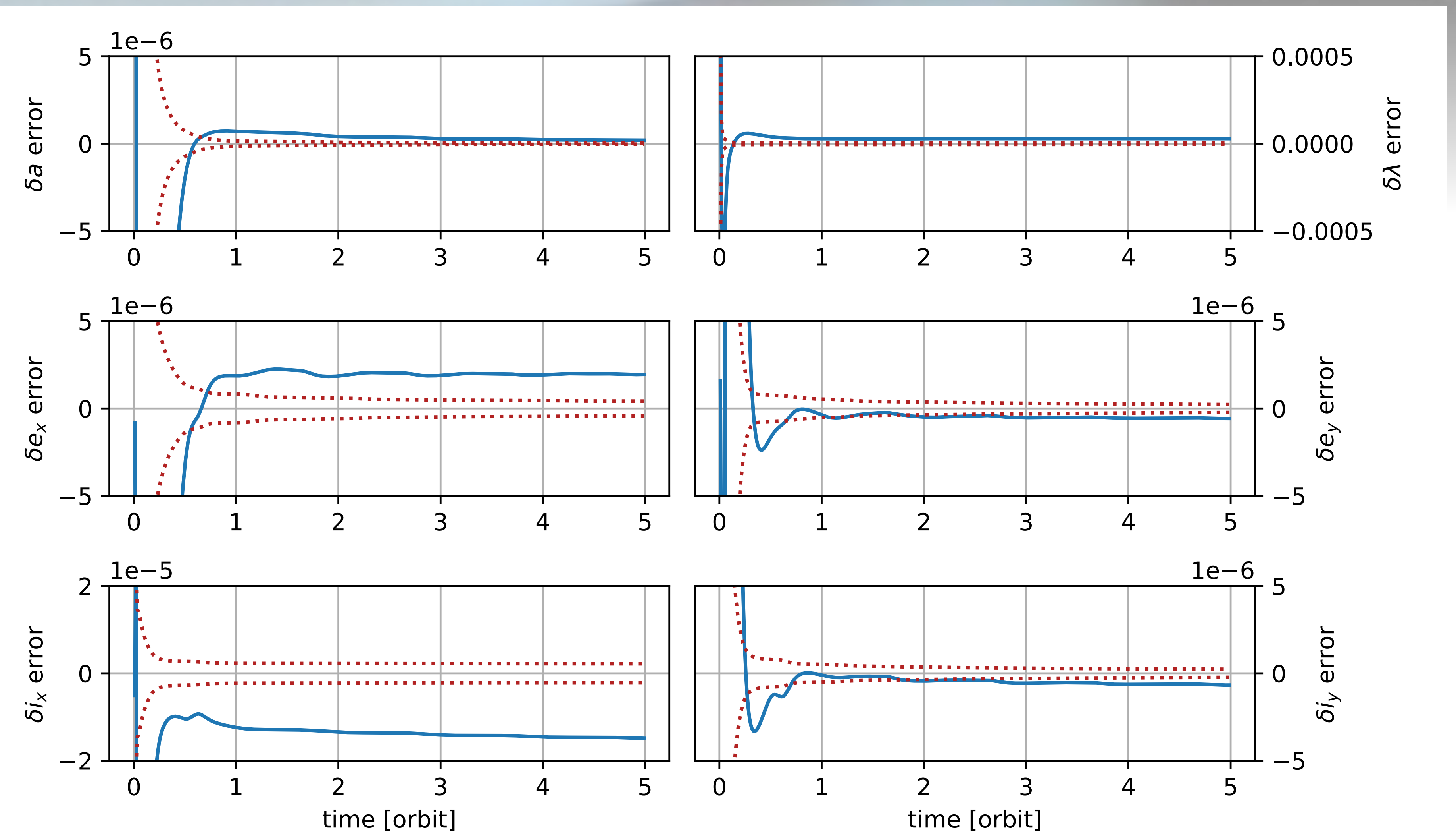

Angles-only ROE:

- Linear dynamics → unobservable
- Non-linear dynamics → weakly observable

Unscented Kalman filter

Dynamics: LPE for J2

Measurements: azimuth-elevation

→ Mean to osculating transformation

Estimated bearing angles

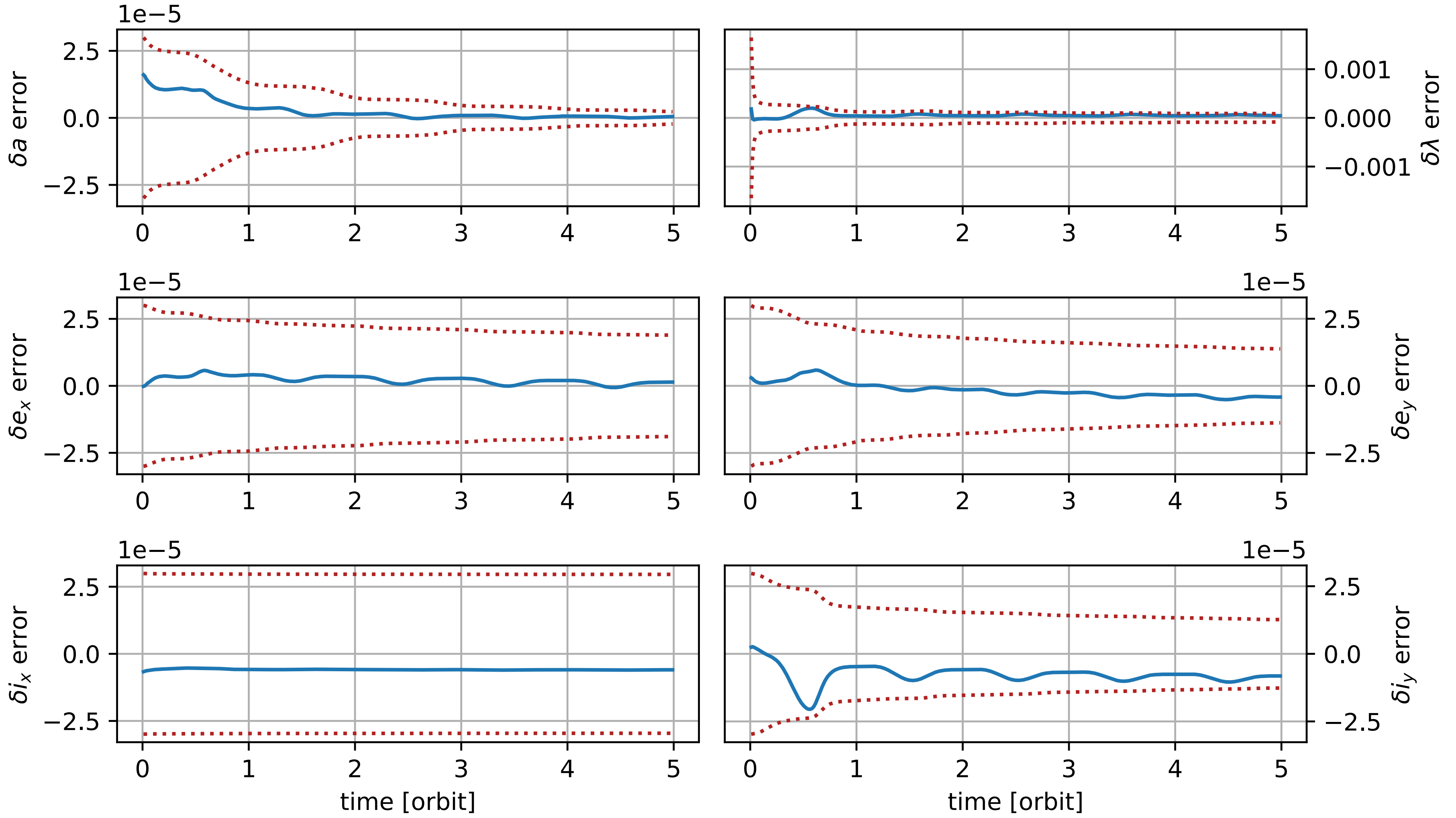

Perfect bearing angles measurement
→ errors / divergence?

Relative Orbit Estimation: Case 1

Angles-only ROE:
- Linear dynamics → unobservable
- Non-linear dynamics → weakly observable

Unscented Kalman filter

Dynamics: LPE for J2

Measurements: azimuth-elevation

→ Mean to osculating transformation

→ Brouwer-Lyddane transformation (order J2 ~1e-6)

Perfect bearing angles

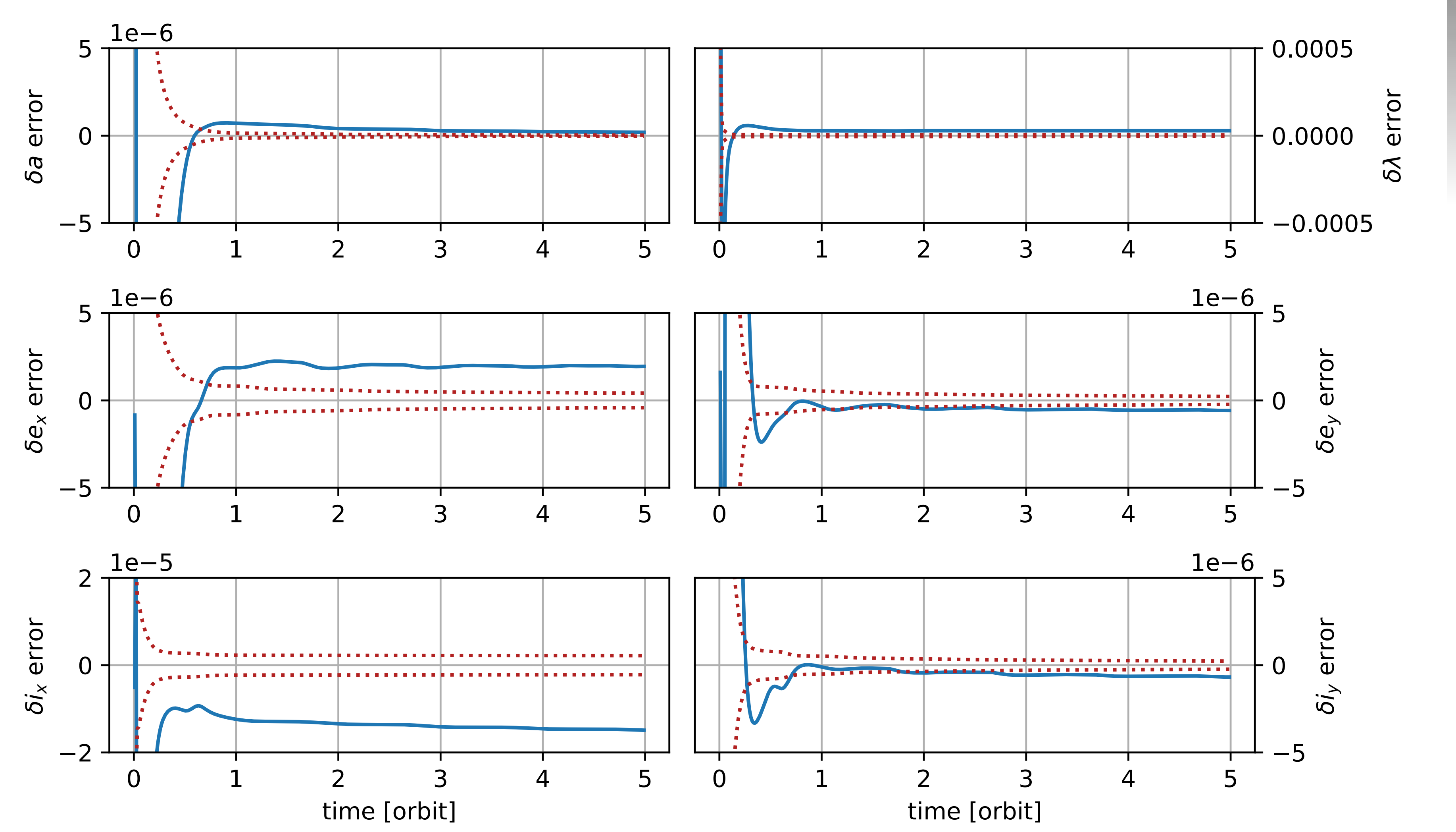

Estimated bearing angles

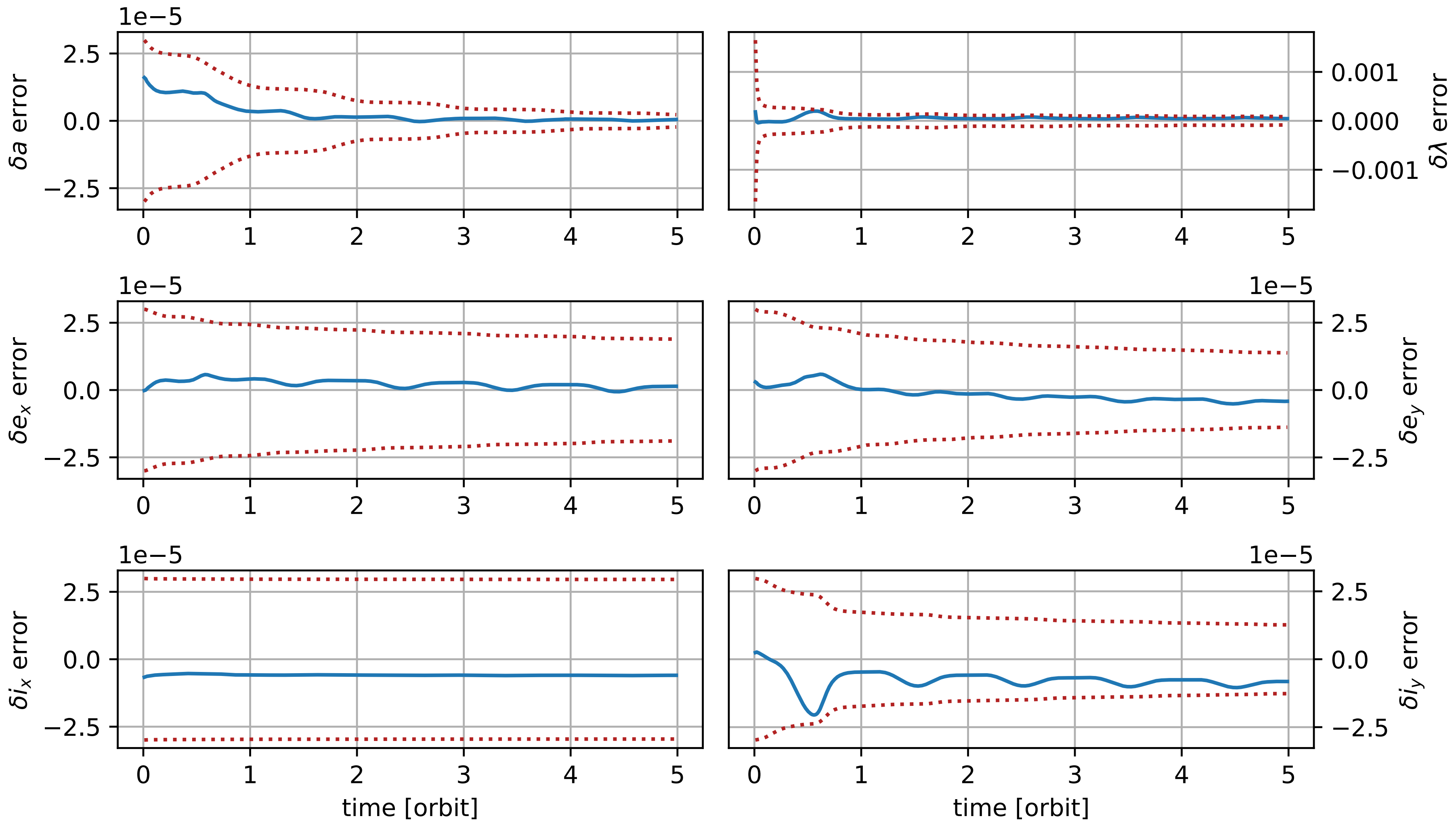

Relative Orbit Estimation: Case 2

Perfect bearing angles

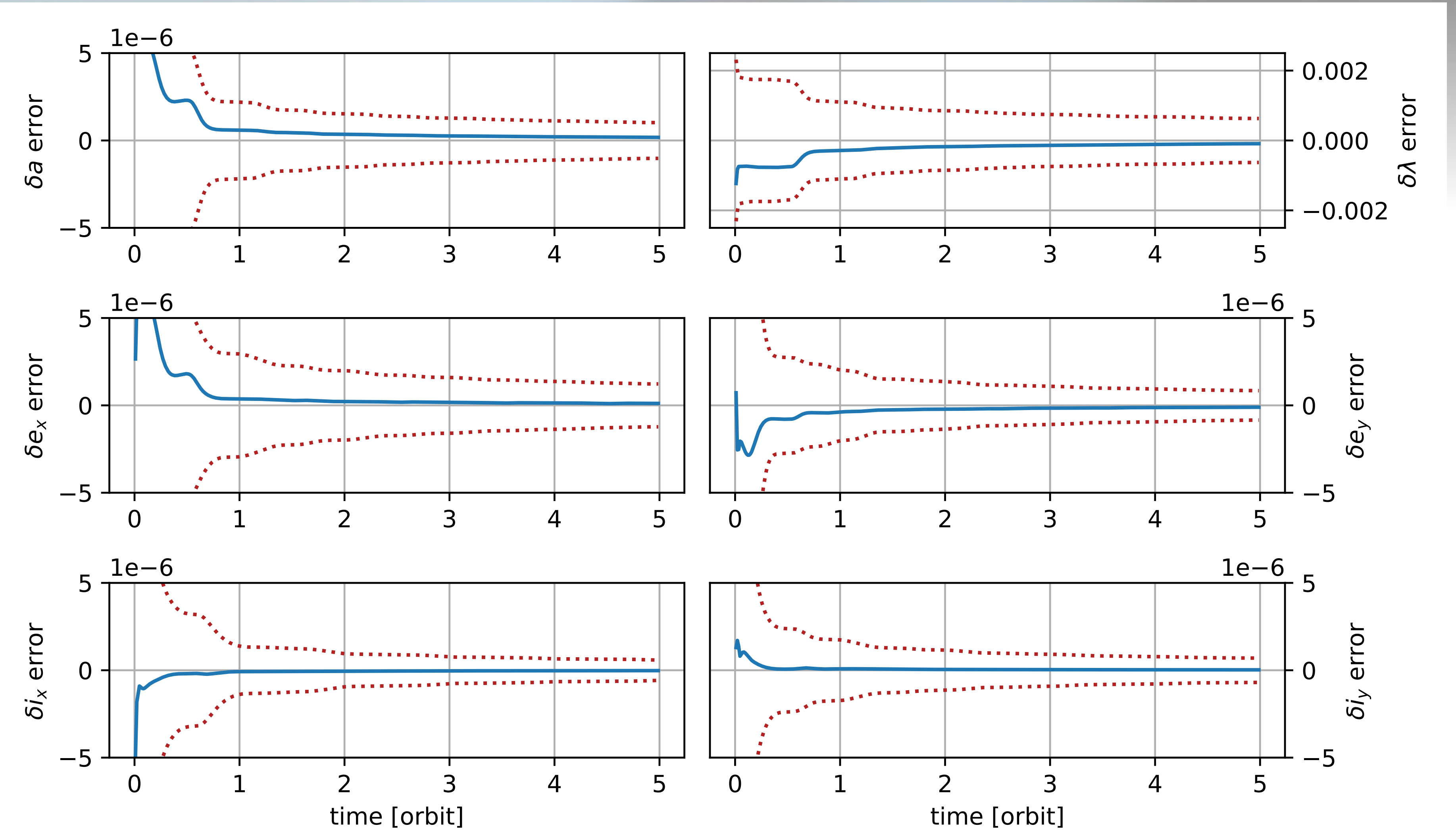

Angles-only ROE:

- Linear dynamics → unobservable
- Non-linear dynamics → weakly observable

Unscented Kalman filter

Dynamics: LPE for J2

Estimated bearing angles

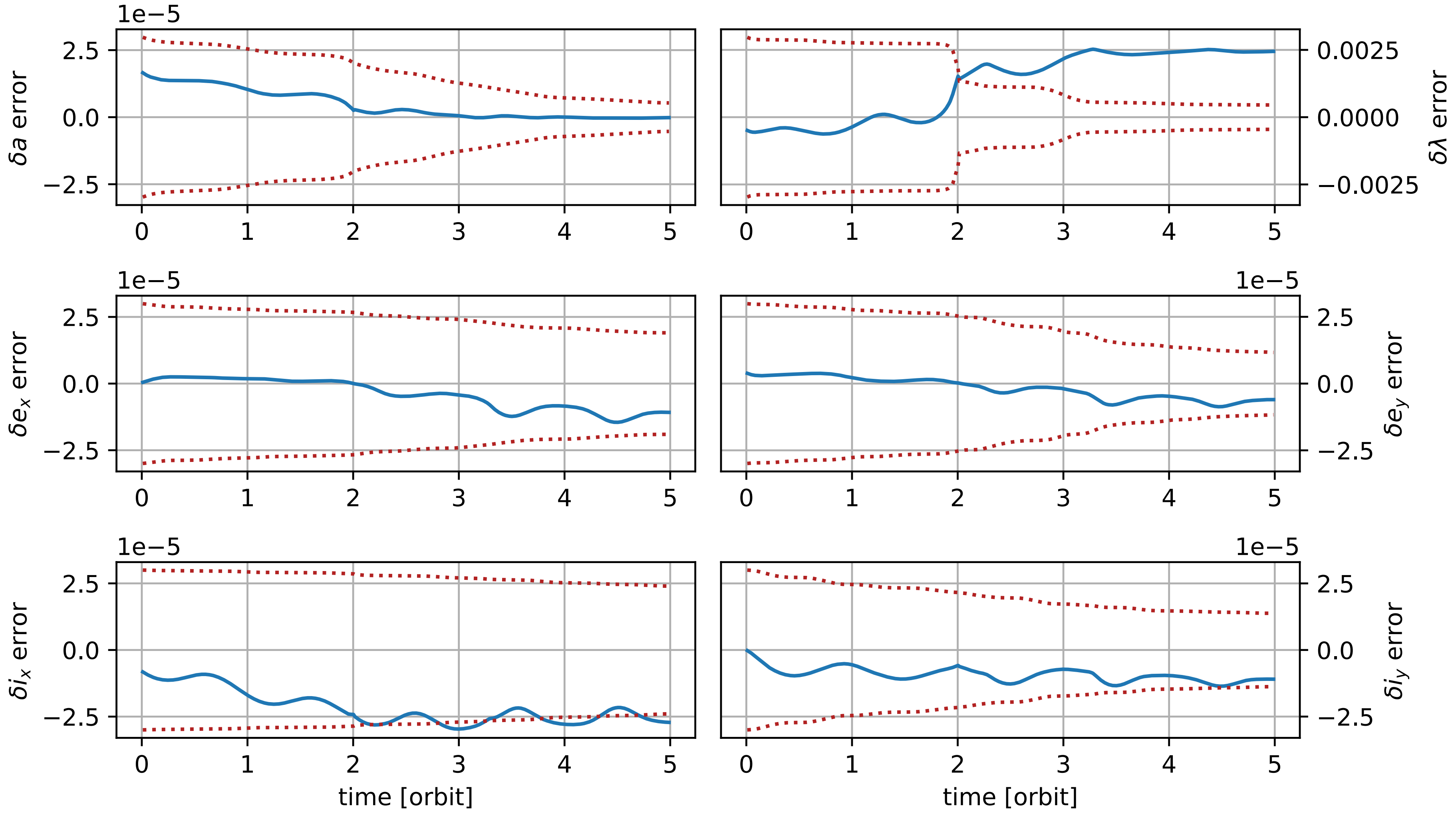

Measurements: azimuth-elevation

→ Mean to osculating transformation

→ Brouwer-Lyddane transformation (order J2 ~1e-6)

Relative Orbit Estimation: Residuals Case 1

Perfect bearing angles

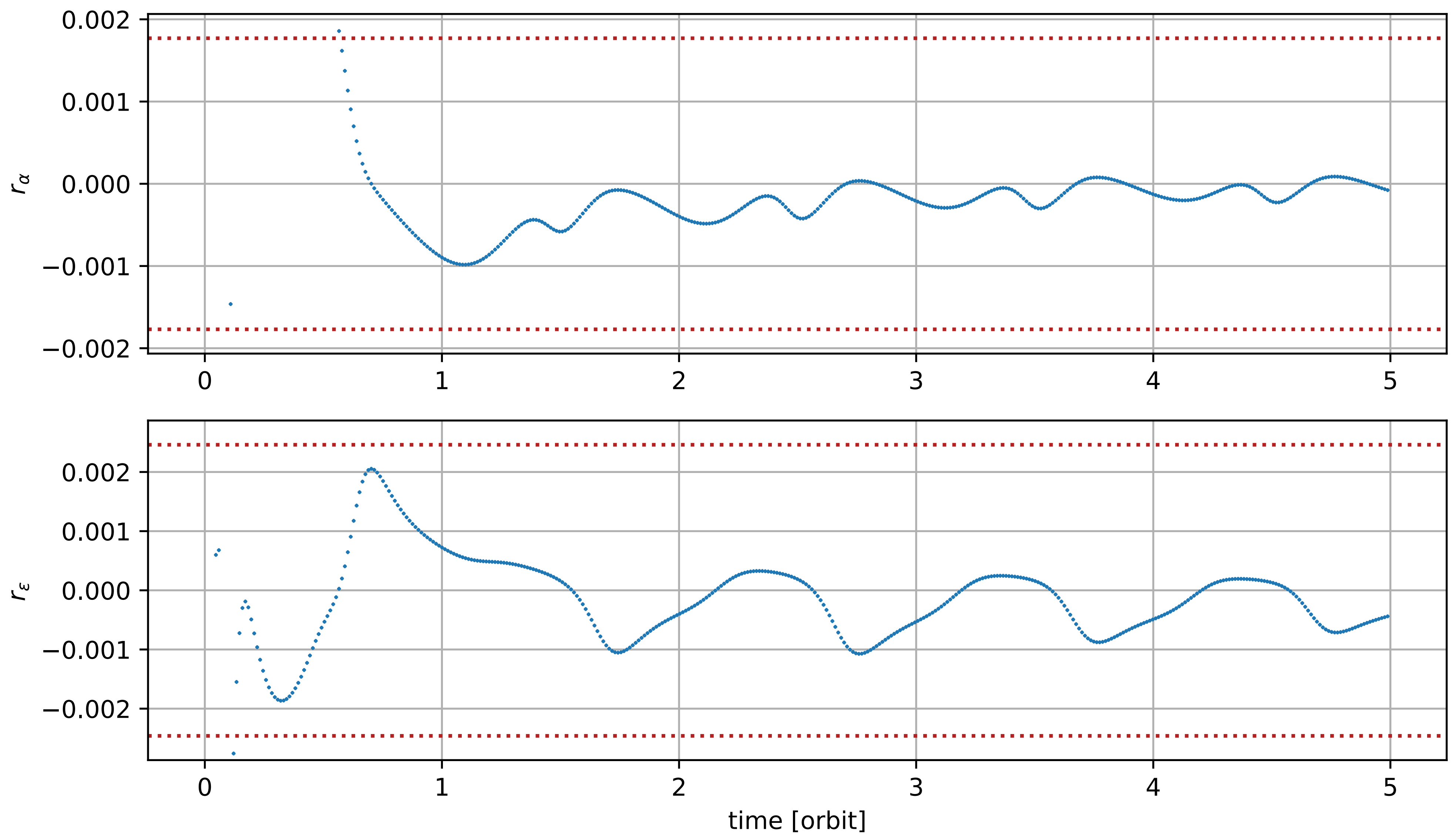

Estimated bearing angles

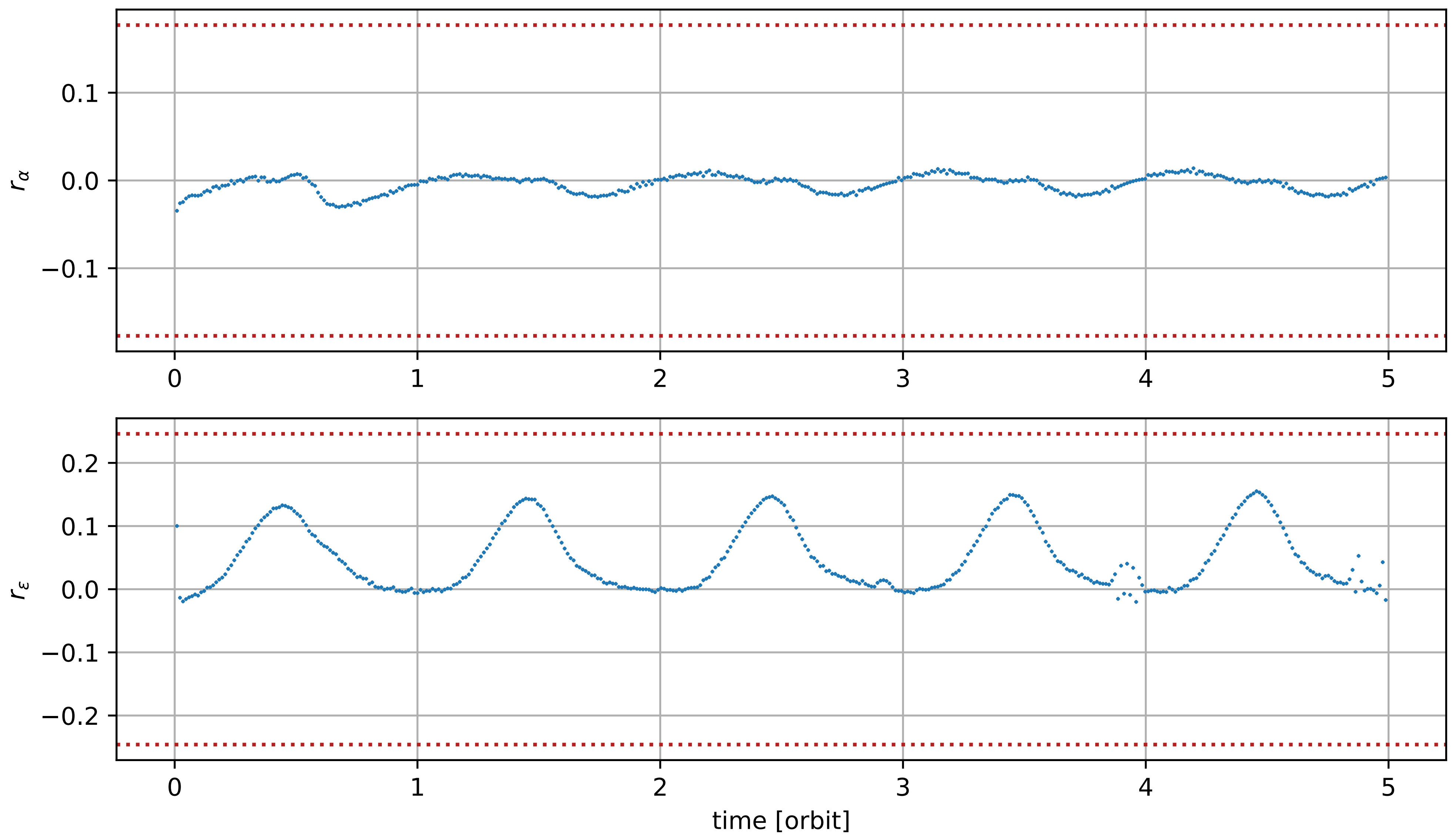

B-L structure → Repeatability with orbit period

Conclusions

- Setup
  - Assembly of off-the-shelf x-ray sensors
  - On/off signals
  - Rotating platform
  - Moving target → relative orbit
- Relative Orbit Estimation
  - Pre-processing: Batch least-squares → "angles-only"
  - Unscented Kalman filter
- Future work
  - Estimation problem: observability study, process noise model
  - SNR analysis for different plasma environments in regions of interest

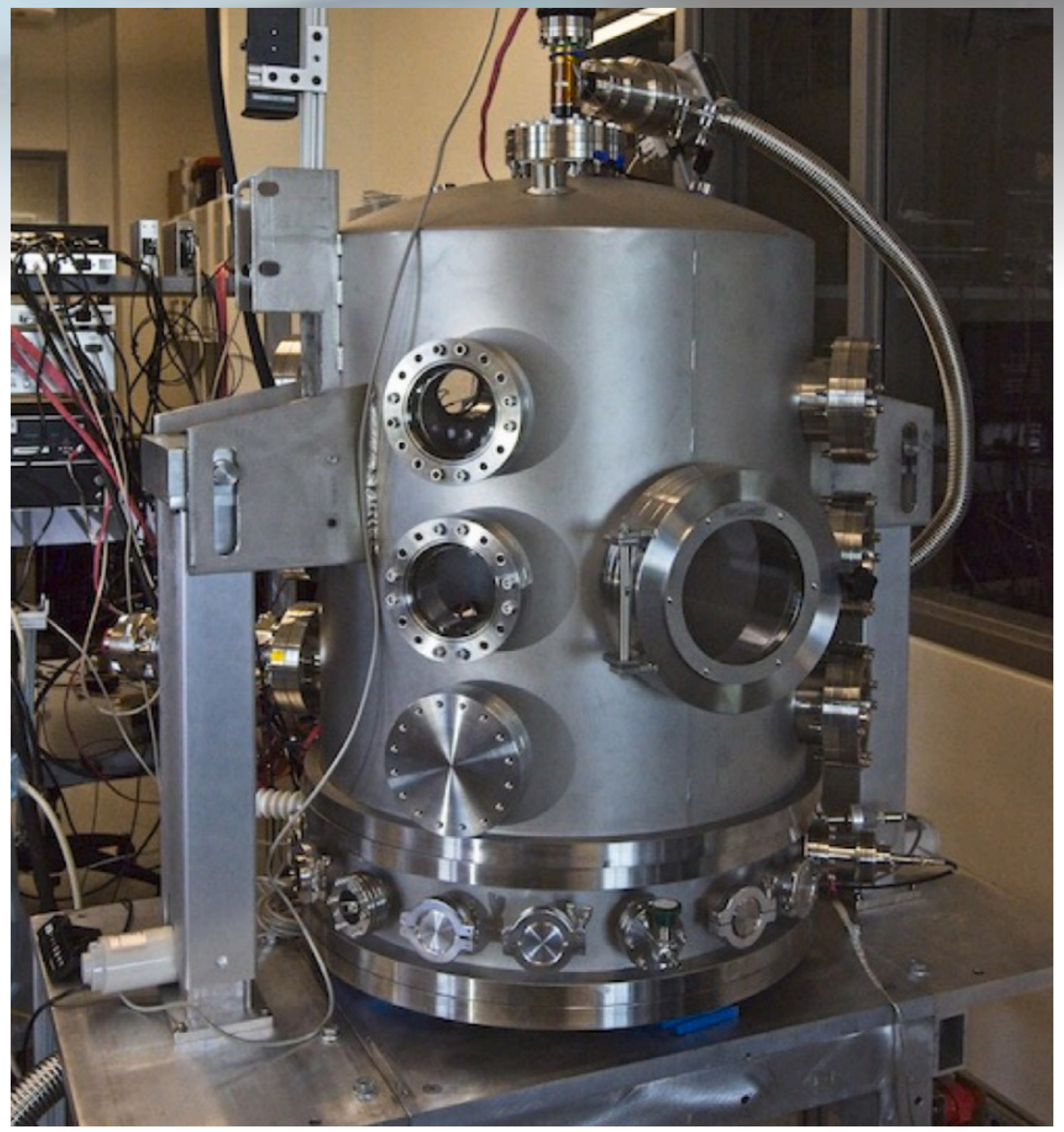

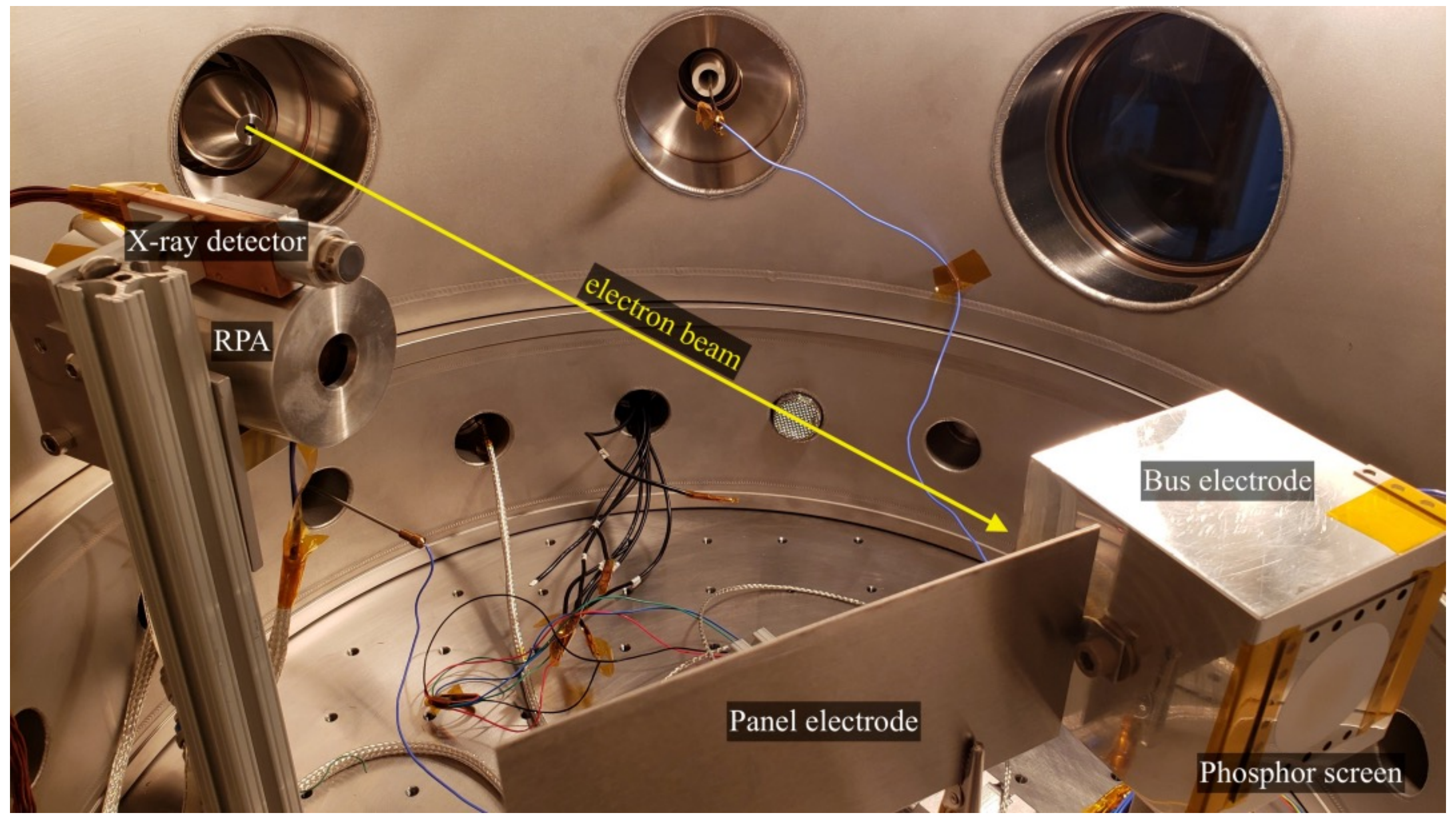

Electrostatic Charging Laboratory for Interactions between Plasma and Spacecraft (ECLIPS) research vacuum chamber

Questions?

andrea.lopez@colorado.edu

AVS Lab website: http://hanspeterschaub.info/main.html

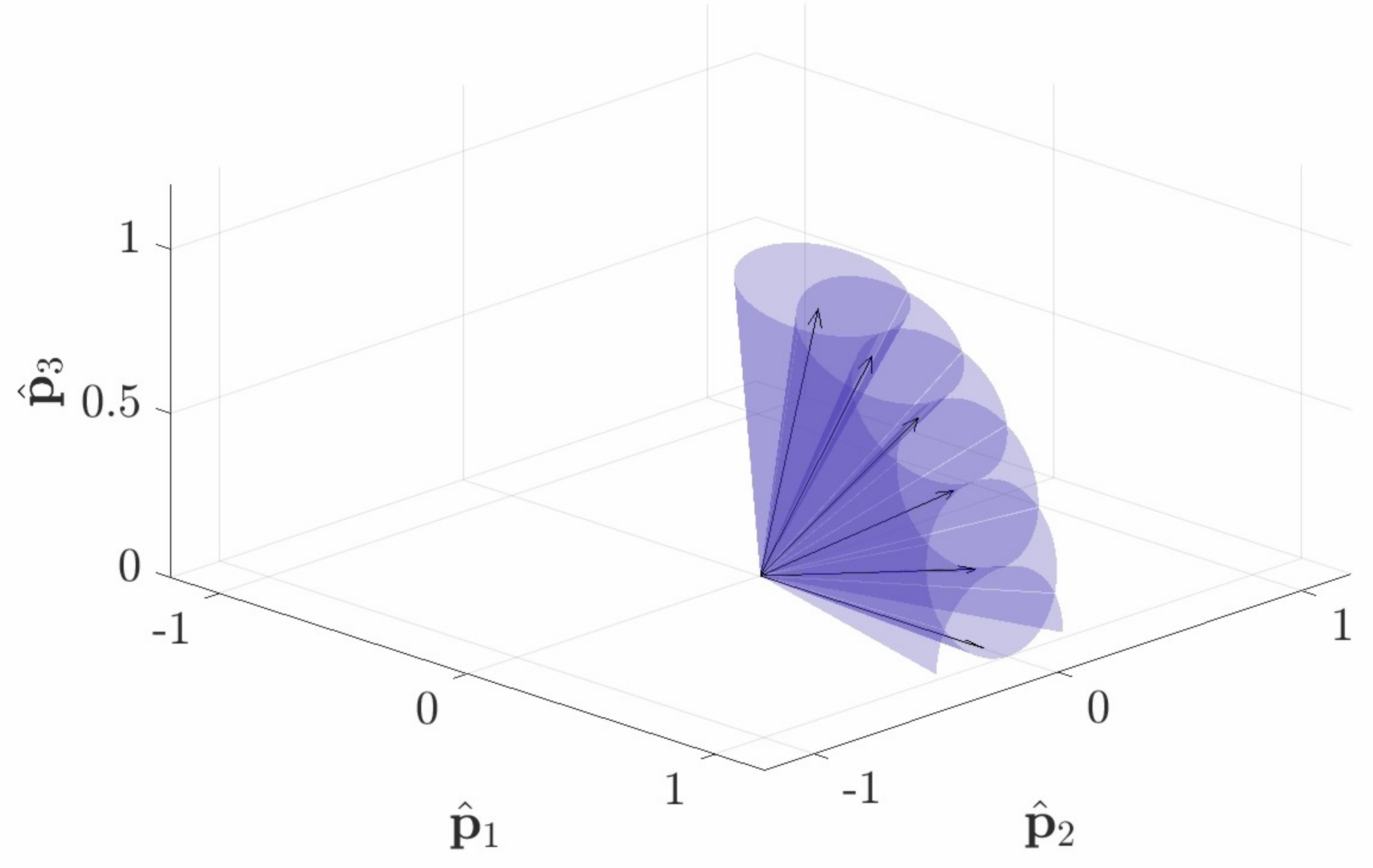

Acknowledgements:

This work was supported by the U.S. Air Force Office of Scientific Research under grant FA9550-23-1-0570.

Backup slides

Electron plasma parameters in Cislunar

Region	Altitude [km]	Mean Electron Temperature [eV]	Max. Electron Temperature [eV]
Magnetotail lobes	>100	48	980
Plasma Sheet	>100	150	3700
Magnetosheath Dayside	>100	18	1400
Magnetosheath Wake	100-2000	50	840
	2000-12000	19	920
	>12000	17	710
Solar Wind Dayside	>100	11	126
Solar Wind Wake	100-500	60	430
	500-2000	50	350
	2000-12000	29	220
	>12000	19	64

NASA Cross-Program Design Specifications for Natural Environments (DSNE), Rev I

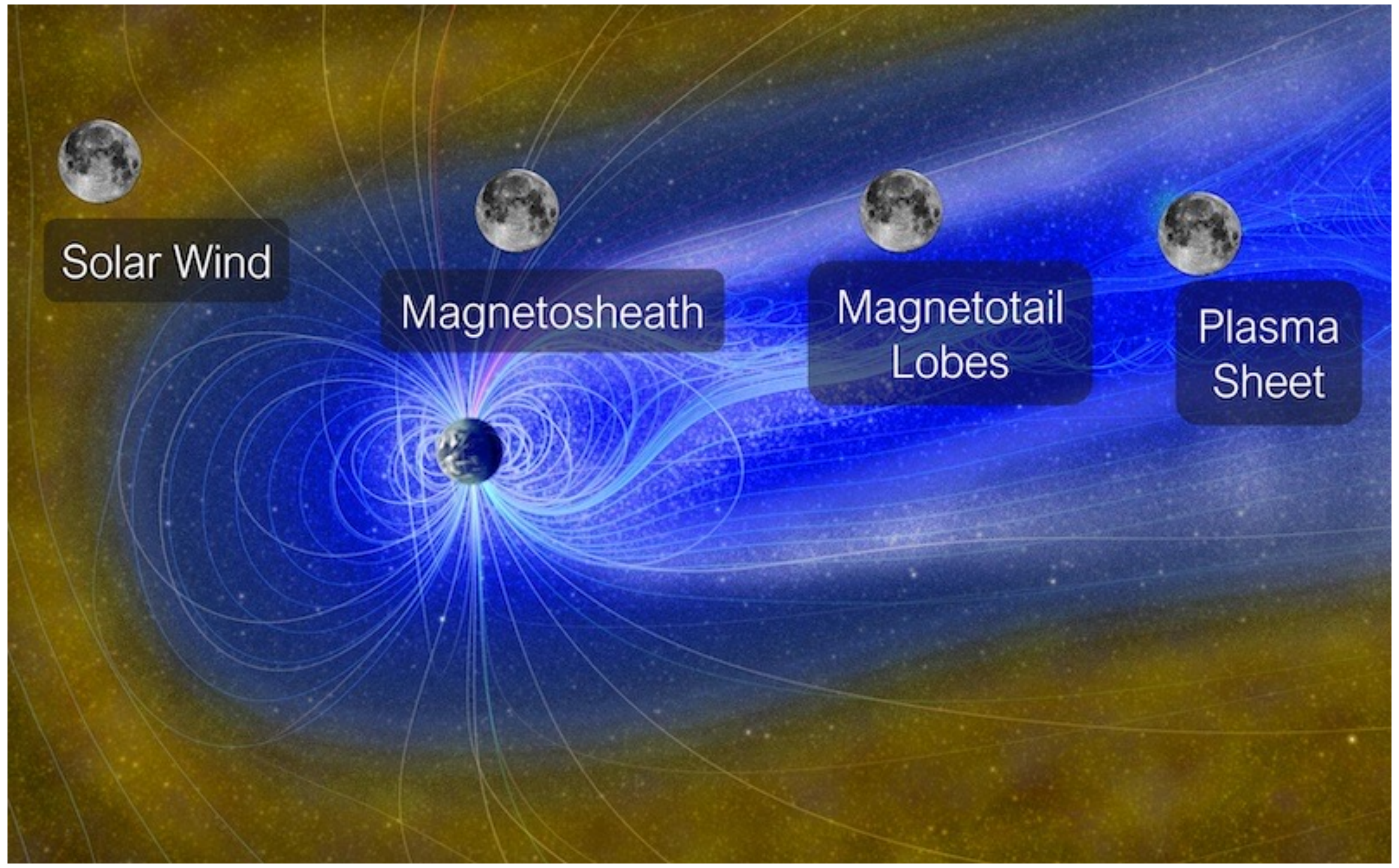

Credit: Kaylee Champion

Electron plasma parameters in Cislunar

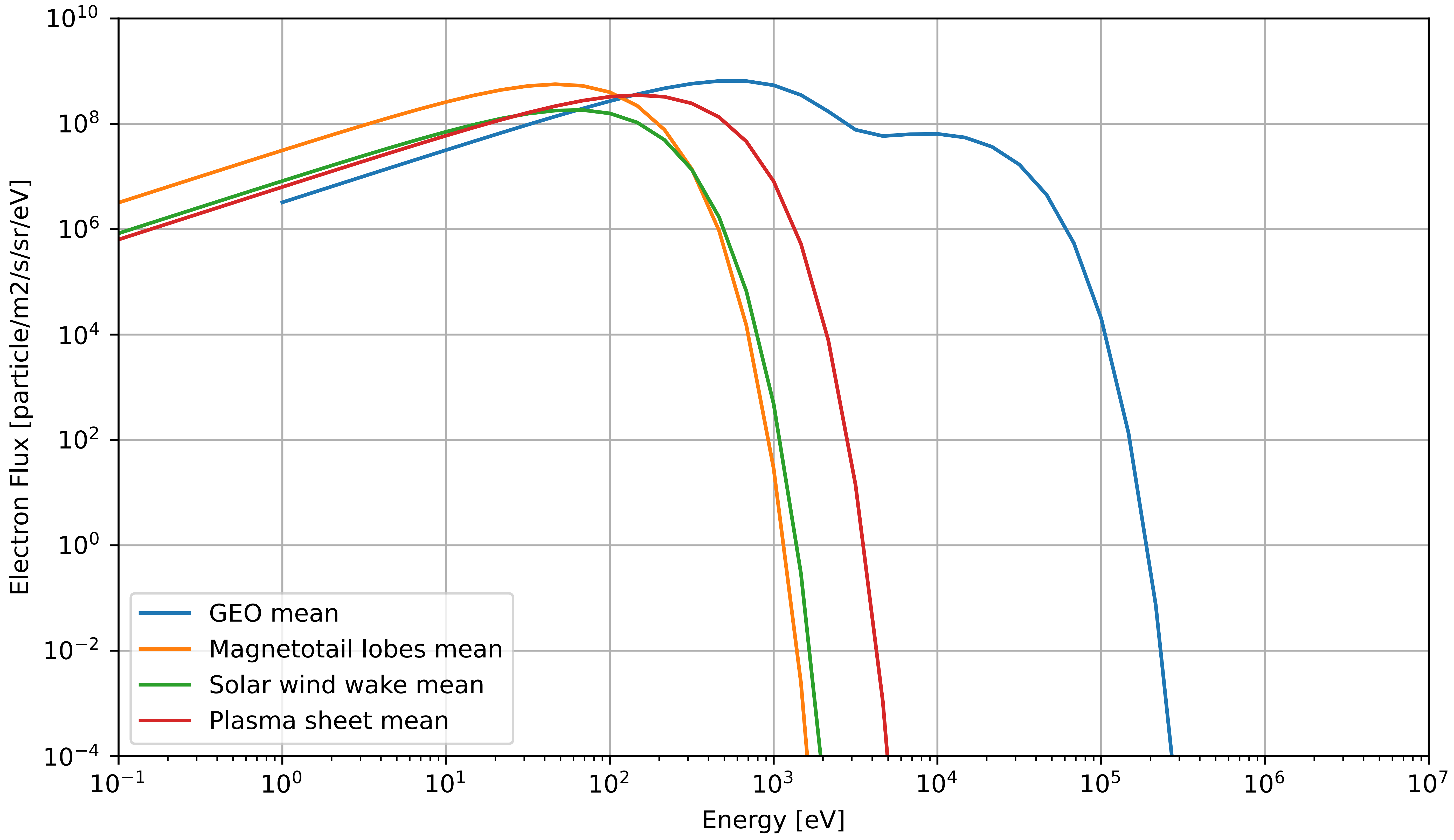

Hill frame estimation errors: Case 1

Perfect bearing angles

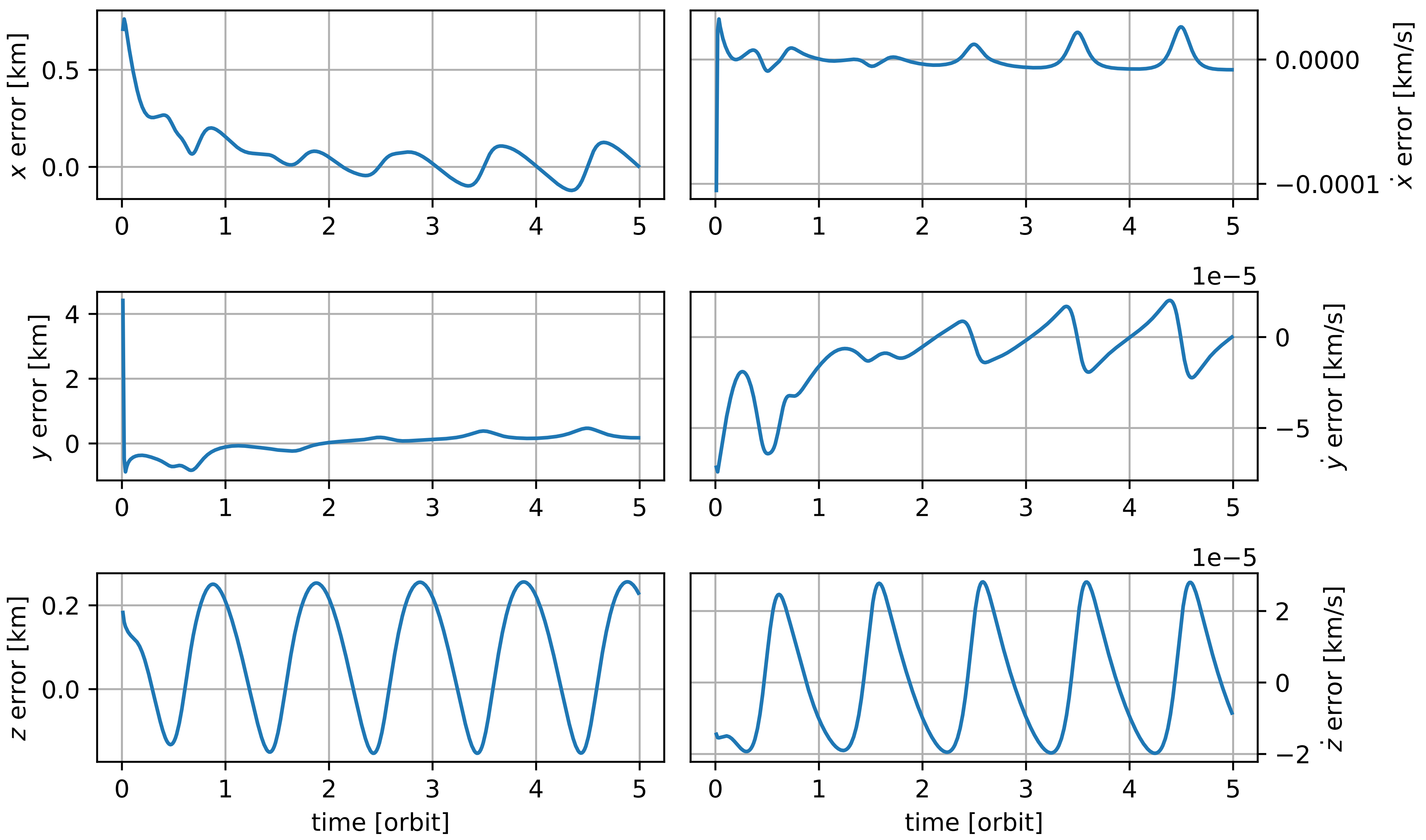

Estimated bearing angles

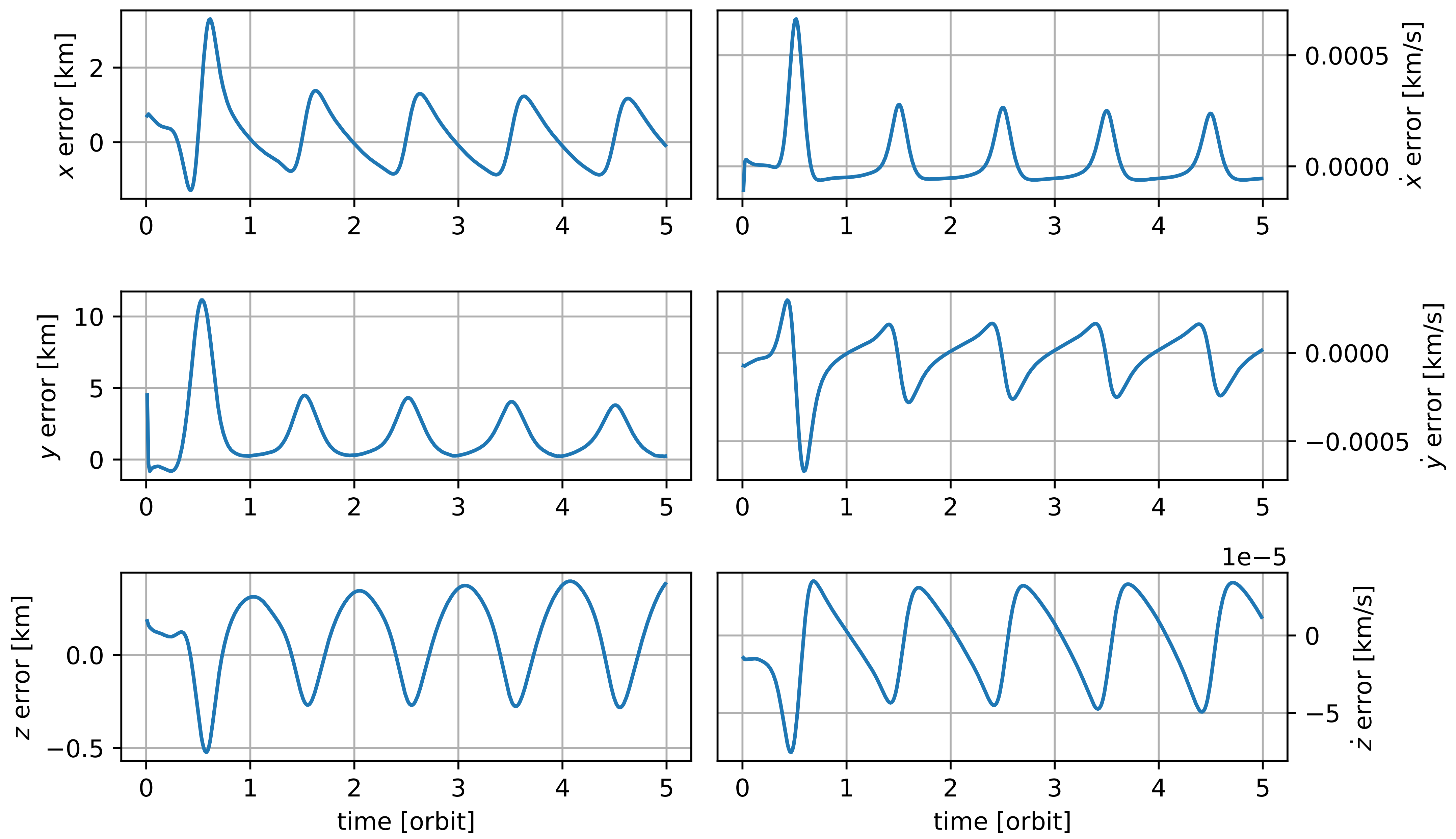

Hill frame estimation errors: Case 2

Perfect bearing angles

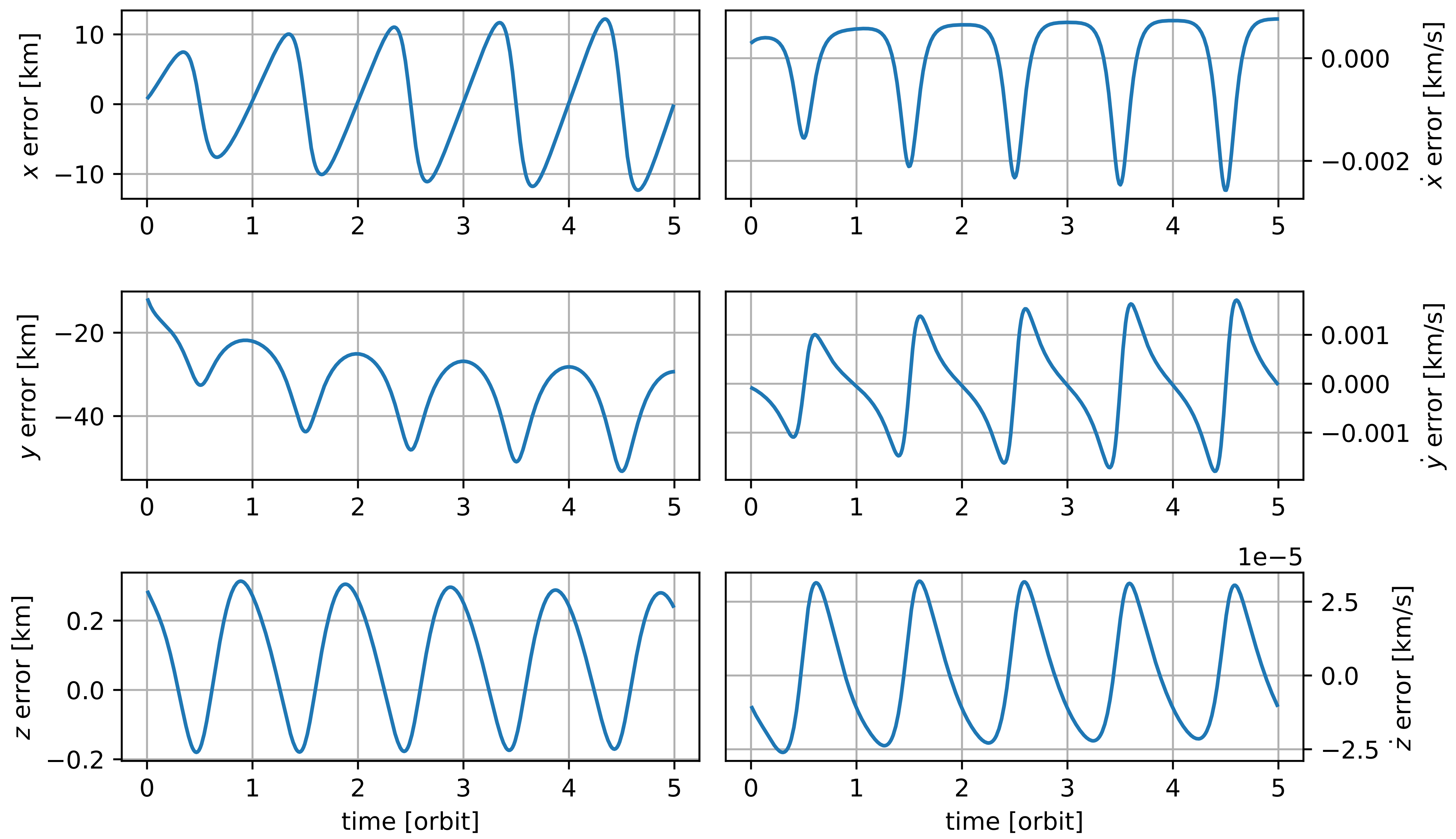

Estimated bearing angles